Divergent medial amygdala circuits for resolving approach-avoidance conflict

Samara Maxine Miller

A dissertation

submitted in partial fulfillment of the

requirements for the degree of

Doctor of Philosophy

University of Washington

2018

Reading Committee:

Larry Zweifel, Chair

Stanley McKnight

John Neumaier

Program Authorized to Offer Degree:

Pharmacology

University of Washington

Abstract

Divergent medial amygdala circuits for resolving approach-avoidance conflict

Samara Maxine Miller

Chair of the Supervisory Committee:

Larry Zweifel

Department of Pharmacology

Avoidance of innate threats is often conflicted by motivations to engage in exploratory approach behavior. The neural circuits that underlie this approach-avoidance conflict are not well resolved. Here, we isolated a population of dopamine D1 receptor (D1R) expressing neurons within the posteroventral region of the medial amygdala (MeApv) in mice that are activated either during approach or during avoidance of an innate threat stimulus. Distinct subpopulations of MeApv-D1R neurons differentially innervate the ventromedial hypothalamus (VMH) and bed nucleus of the stria terminalis (BNST) and these projections have opposing effects on investigation or avoidance of threatening stimuli. These circuits are potently modulated through opposite actions of D1R signaling that bias approach behavior. These data demonstrate divergent

pathways in the MeApv that can be differentially weighted towards exploration or evasion of threats.

Table of Contents

Chapter 1: Introduction

An important aspect of behavioral responses to threatening stimuli is the ability to modulate defensive actions, either enhancing or suppressing these behaviors depending on environmental demands or changing internal central motive states. A major conflicting drive of innate avoidance is an inherent motivation to approach and explore the unknown. In the classical sense of approach-avoidance conflict, exploratory drive is an essential feature of maximizing an animal's ability to thrive, whereas avoidance is an essential feature of survival[1] The approach-avoidance perspective is a useful framework for integrating our understanding of cognitive processes and behavioral output. In particular, the approach and avoidance distinction provides an important context for understanding various domains of motivation in healthy and pathological states. Avoidance is a central symptom of anxiety disorders such as posttraumatic stress disorder (PTSD), panic disorder and social anxiety disorder (SAD)[2]. Thus, understanding the neural correlates of approach and avoidance processes will thus enhance our insight into the dysfunctions associated with these disorders.

Approach and avoidance

The distinction between approach versus avoidance motivation is perhaps one of the most basic and fundamental concepts describing an organism's behavior. Philosophers and scholars have observed it for centuries, whether through the philosopher Jeremy Bentham's characterization of hedonism and the pursuit of pleasure

over pain, or within the context of the psychologist Ivan Pavlov's description of reflexive responses in which a subject orients either toward or away from stimuli[3,4]. The diversity of conceptualizations of approach-avoidance perspectives throughout academic history is a testament to its importance to human functioning. Indeed, both approach and avoidance are critical for adaptation and survival: avoidance of aversive stimuli facilitates surviving, and approach of appetitive stimuli facilitates thriving[1].

In the field of psychology, approach is defined as the energization or direction of behavior toward an appetitive stimulus, such as food or a mate[1]. Avoidance is characterized by energization or direction of behavior away from an threatening stimulus, such as a predator or an aggressive conspecific[1]. Approach and avoidance are not only relevant to human behavior, but underlie adaptive decision making in organisms across all animate life. The animal psychologist T.C Schneirla argued that all organisms rely on approach-based mechanisms to obtain food, shelter and mates, and avoidance-based mechanisms to effectively defend and protect against threats[5]. The amoeba, for example, contains a simple reflexive approach-avoidance mechanism that enables it to move away or toward varying intensities of light sources through contractions and expansions in its protoplasm[5]. In mammalian species, approach-avoidance mechanisms can be as simple as a reflexive startle response[6], or as complex as cortical processes that evaluate the relative risk or reward of a potential action[7]. Across all of these systems, the organism's survival depends heavily on its ability to accurately determine the beneficial or harmful potential of environmental stimuli and make subsequent decision to approach or avoid it.

Given that approach and avoidance mechanisms are fundamental and ubiquitous regulators of animal behavior, they provide a unique framework for understanding motivation and decision making more broadly. While the field of psychology has made strides to employ the approach-avoidance distinction as a platform for dissecting motivation, less is known about the neural substrates underlying the mechanisms of approach-avoidance. Nonetheless, there have been a number of both human and rodent studies looking at brain regions involved in basic approach and avoidance behaviors.

Researchers have employed several decision-making paradigms associated with discriminating between the value of good and bad stimuli to study approach-avoidance behavior. In rodents, many approach-based behavioral paradigms rely on an animal's passive experience of appetitive stimuli such as food or social interactions, whereas avoidance-based paradigms test an animal's passive experience of fear-producing stimuli such as aversive smells or sounds[8]. In particular, approach-avoidance mechanisms are often studied in the context of the predator defense, or fear, system because stimuli associated with predators/threats elicit robust behavioral responses[9]. Brain regions so far implicated in defensive responses to predator stimuli are therefore considered here as likely candidates underlying the neural basis of approach-avoidance behavior.

Brain regions involved in approach-avoidance

Many classical studies used lesion and electrical stimulation protocols to identify brain regions involved in approach-avoidance interactions. Research from the mid '50s and '60s, pioneered by the Olds and Blanchard groups, demonstrated that electrical

manipulations of the hypothalamus, ventral tegmental area and amygdala of rodents evoked both positive reinforcement (approach) as well as escape (avoidance) behavior[10-13]. Initial studies presented conflicting data regarding how different manipulations affected the direction of this behavior. For example, some suggested that stimulation of the hypothalamus elicited strictly avoidance[14], while others suggested stimulation generated approach behavior[15]. Efforts to resolve this have been impeded by the challenge of genetically dissecting these regions; however, early studies provided interesting clues as to the role of the hypothalamus, and in particular, the amygdala in the regulation of approach and avoidance.

In 1967, Olds and Olds used stimulating electrodes systematically placed throughout the rat brain and characterized behavior depending on whether or not the animal more readily approached or avoided electrical self-simulation of various target structures (specifically, levers that produced electrical stimulation)[10]. Their studies demonstrated that many the brain regions previously implicated in approach and avoidance behavior in fact produced “ambivalent responses”. They suggested that there was a very low likelihood of finding “pure” effects in any one nucleus[10]. While in many ways this study preserved and reinforced the idea that the hypothalamus and amygdala were critical brain regions involved in approach and avoidance, it also revealed the limitations of electro-stimulation experiments for clearly illuminating the specific function of these regions in behavioral regulation. One interesting conclusion to draw from their study is that there are sub-regions and cell types within the larger target structures that are differentially involved in either approach or avoidance. A study from the Blanchard group just a few years later was able to restrict lesions to the corticomedial amygdala in

rats and demonstrated that this almost completely eliminated freezing behavior in response to an immobilized cat, a natural predator to rats[16]. Concurrently, lesions of this area reduced avoidance behavior, including increased exploration of the cat[16₂]. This finding supported the idea that innate approach of the cat is actively suppressed by the avoidance impulse. Together these studies set the stage for highlighting the amygdala as a primary brain region involved in the regulation of basic approach and avoidance behaviors.

The amygdala

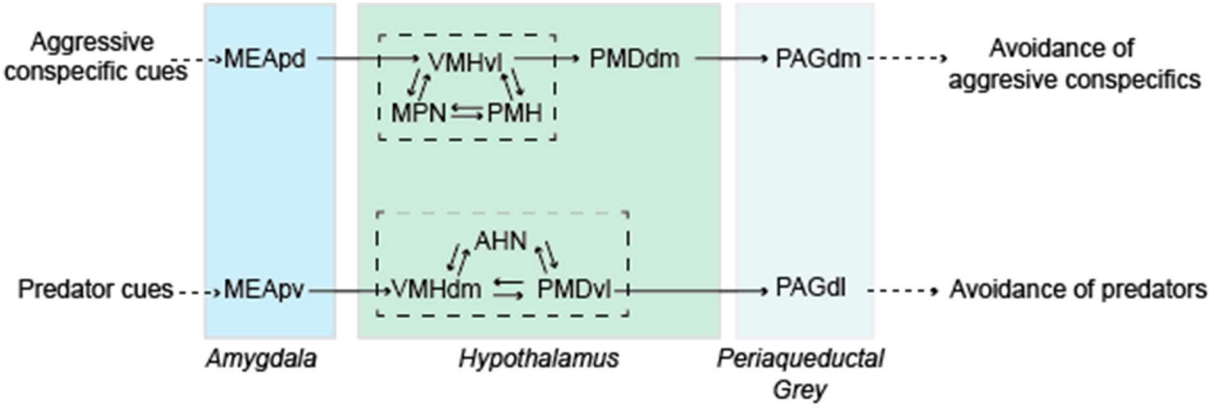

Figure 1: Canonical view of circuit organization of threat processing (adapted from Gross and Canteras 2012)

The amygdala is a complex, heterogeneous structure that is well known for its role in a variety of behaviors related not only to approach-avoidance, but fear and social behaviors as well[17]. The range of these behaviors reflects the heterogeneity of the amygdala, both in its structural make up and cellular composition. A number of studies have investigated these discreet sub-regions and cell populations. A recent review by Gross and Canteras summarized the current view of how these sub-regions are implicated specifically in innate threat behaviors (Figure 1)[18]. The review draws on studies involving classical lesion manipulations as well as c-*fos* experiments that largely

implicate the medial nucleus of the amygdala (MEA) as a critical node regulating approach and avoidance. Broadly, threatening cues are conveyed through sensory input to distinct nuclei within the MEA, whose projections to the hypothalamus ultimately activate regions of the PAG to evoke stimulus- specific defensive responses[18]. Early studies using neural activity mapping and anatomical tracing suggest that distinct types of innate fear behaviors segregate at the level of the projections from the medial nucleus of the amygdala (MEA) to the ventromedial hypothalamus (VMH). Specifically, it is thought that the posterodorsal and posteroventral subdivisions of the MEA (MEApd and MEApv, respectively) are differentially involved in defensive responses to either conspecifics or predators. The MEApd is robustly activated in rodents exposed to aggressive conspecifics[19], while the MEApv is strongly activated in rodents exposed to an innate predator or its odor[20]. Retrograde tracing and *c-fos* expression analysis revealed that MEApv neurons that were activated by threat stimuli projected to hypothalamic nuclei implicated in both appetitive and aversive behaviors[21₆]. In contrast, MEApv neurons activated by reproductive stimuli did not project to these regions[6]. Based on these observations, it was hypothesized that the medial amygdala-hypothalamic circuit may be an important “gate” between conflicting appetitive behavior and threatening stimuli, either through interneurons within the VMH or through indirect modulation by the BNST[21₆].

In addition to being functionally dissociable within the MEA, tracing studies reveal that the MEApd and MEApv exhibit anatomical segregation in their axonal projection patterns as well. Anterograde tracing studies have demonstrated that the MEApd projects to regions implicated in reproduction and conspecific responsive behavior,

including the ventrolateral VMH (VMHvl)[22]. In contrast, the MEApv projects to distinct hypothalamic nuclei involved in predator-responsive defensive behavior including the dorsomedial VMHdm[22]. These striking anatomical differences likely underlie the functional distinctions between the MEApd and the MEApv.

Differential neural activity mapping and anatomical segregation of MEA-VMH pathways suggests that conspecific and predator responsive defensive behavior may be processed through independent amygdalar-hypothalamic circuits. Recent advances in genetic technology have enabled the isolation of specific cell types within these nuclei to functionally dissect the neural circuits underlying behavior. These studies have primarily focused on the role of the VMH and MEApd in regulating aspects of innate defensive behavior. Genetic manipulations of the VMH have shown that optogenetic stimulation of the VMHvl evokes aggressive behavior, whereas stimulation of the VMHdm promotes freezing, avoidance and defensive behaviors[23,24]. Interestingly, optogenetic mapping revealed a unique microcircuitry within the VMH showing that neurons within the central VMH (VMHc) strongly excite the VMHvl neurons to drive behavioral aggression[25]. Cell-specific manipulations of distinct neuronal populations in the MEApd revealed that a GABAergic subpopulation promotes aggression, mating and social grooming, while separate glutamatergic neurons in the MEApd promote asocial self- grooming behavior[26]. Aromatase-positive neurons specifically located in the MEApd have also been shown to regulate specific components of aggression in both males and females[27]. In recent years, studies looking at behavioral regulation through the MEA have focused on the MEApd. However, there has been very little genetic dissection of the MEApv and its functional

role in approach-avoidance mechanisms, largely because there has yet to be a good genetic marker for this discrete nucleus.

Beside its regional and circuit segregation, the MEA also possesses rich cellular heterogeneity. Recent studies investigating the electrophysiological properties of the MEA demonstrated that there are largely GABAergic neurons within the MEApd and non-GABAergic neurons within the MEApv[28,29]. Within the MEApd, there are localized populations of the transcription factor Lhx6[21], as well as a discretely localized population of aromatase neurons[27]. The MEApv, despite being less studied, expresses the transcription factor Lhx9[21]. The unique cellular heterogeneity within the MEA merits further exploration for understanding how different MEA neuronal subtypes regulate discrete domains of approach and avoidance behavior.

Despite what is known about the amygdala and its role in innate defensive behaviors, there are still many open questions within the field, especially in regard to the role of the MEApv. Additionally, given the proposed parallel circuit organization between the MEApd and MEApv and their functional distinctions, it begs the question about how an animal makes adaptive decisions when faced with conflicting cues in their environment. One possible explanation for this is that neuromodulators, such as dopamine or acetylcholine, signal within this brain area to bias behavioral responses depending on factors such as the valence of a stimuli, or an organism's motivational state.

Dopamine

In an approach-avoidance scenario, the valuation of a stimulus is a dynamic process related to the internal state of an organism, as well as complex environmental

variables. Avoidance and approach mechanisms are a powerful example of how organisms engage flexible decision making strategies to integrate fluctuations in internal and external landscapes. As such, animals must often make trade-offs between competing motivational drives. For example, studies have shown that a hungry animal will overcome its fear of a predator cue in order to access food[30]. Researchers hypothesize that neuromodulators such as dopamine (DA) and acetylcholine (ACh) are involved in this behavior[31]. In fact, there is a growing amount of evidence implicating DA as a neural substrate for approach mechanisms. The midbrain dopamine system plays an essential role in reward learning, motivation, fear learning and avoidance of conditioned stimuli[32][8]. In the canonical view of the dopamine system, tonic dopamine levels rise in response to environmental stimuli to maintain a 'ready' state that allows an animal to respond to a variety of external stimuli[33]. In contrast, phasic increases in dopamine promote reinforcement, action selection, and incentive motivational processes[8]. Recent data support a role for dopamine in modulating approach-avoidance conflict resolution. For example, increasing dopamine activity by lesioning the RMTg, a significant inhibitory input onto dopamine neurons in the VTA, causes animals to display increased approach to a predator odor threat[34][10]. Additionally, evidence suggests that increasing dopamine with the use of monoamine oxidase inhibitors is an effective treatment for specific phobias[11], a disorder likely caused by dysfunction in innate fear circuitry[35][12]. While dopamine is more widely appreciated as a "reward" or "approach" signal, there is a growing evidence for the role of dopamine in avoidance behavior as well. Recent studies have shown that DA release may also signal and predict successful avoidance of a shock-paired lever stimulus[36]. Neurotransmitters such as

dopamine are an important physiological mechanism by which an organism can modulate motivational drives to ultimately direct behavior. Although dopamine is likely involved in approach and avoidance behavior, there is no evidence demonstrating how dopamine is acting within the medial amygdala to regulate these behaviors.

Dopamine receptors are expressed broadly throughout the brain, including within the amygdala. Importantly, the effects of DA differ depending on the type of receptor and neuron involved. There are two primary classes of dopamine receptor subtypes including the dopamine 1 (D1) receptors and the dopamine 2 (D2) receptor subtypes. In the canonical view, D1Rs are coupled to the stimulatory G (Gs) protein coupled receptor and increase neuronal activity upon activation[37]. Conversely, D2Rs are coupled to the inhibitory G (Gi) protein coupled receptor and inhibit neuronal activity following ligand binding[37]. Interestingly, the binding properties of DA receptors can also change in response to fluctuations in synaptic physiology, such as increased DA release in the case of approach type behavior such as drug or food seeking[37]. More specifically, many groups have observed inhibitory effects through D1R activation. This inhibition is thought to result from various downstream effects of D1R activation, including a suppression of sodium and calcium currents[38]. One study demonstrated that the inhibitory effects of D1R activation in the basolateral amygdala were due to alternate coupling to G protein-coupled inward rectifier potassium (GIRK) channels leading to hyperpolarization caused by an efflux of potassium[39]. Alternatively, D1R-evoked inhibition may depend on the initial membrane potential of the neuron, such that a neuron at more hyperpolarized resting state would be inhibited by dopamine[38]. This

diversity of DA actions likely contributes to its ability to scale behavioral responses as an animal's motivational state adapts to its changing environment.

While dopamine receptors are known to be expressed throughout the amygdala, the specific expression of DA receptors types in the medial division of the amygdala is not well explored. Given the role of the MEA in processing threatening cues, we hypothesized that isolation of dopamine receptive neurons in the MEA would provide key insights into the regulation of innate approach and avoidance. Here, we identified dopamine receptive neurons in the MEApv that express D1R and demonstrate that these neurons encompass two distinct projections, one largely inhibitory projection to the BNST and one largely excitatory projection to the dorsomedial VMH (VMHdm). These data provide direct support for divergent pathways in the MEApv that can be weighted towards approach in the face of threat and have important implications for neural mechanisms underlying internal state conflict resolution.

Chapter 2: Identification and characterization of dopamine receptive neurons in the MEApv

Introduction

To date, most studies looking at the role of amygdalar dopamine and dopamine receptors focus on the central and basolateral nuclei of the amygdala[40]. For example, infusions of either a D1 antagonist into the CEA[41] or D2 antagonist into the BL[42,43] of rats blunts fear learning during a conditioned fear paradigm. The identification or function of dopamine receptors in the medial nucleus of the amygdala has not yet been investigated. Given the role of the MEA in processing innately threatening cues, we hypothesized that isolation of dopamine receptive neurons in the MEA would provide key insights into the regulation of innate approach and avoidance.

Results

Localization within the MEApv

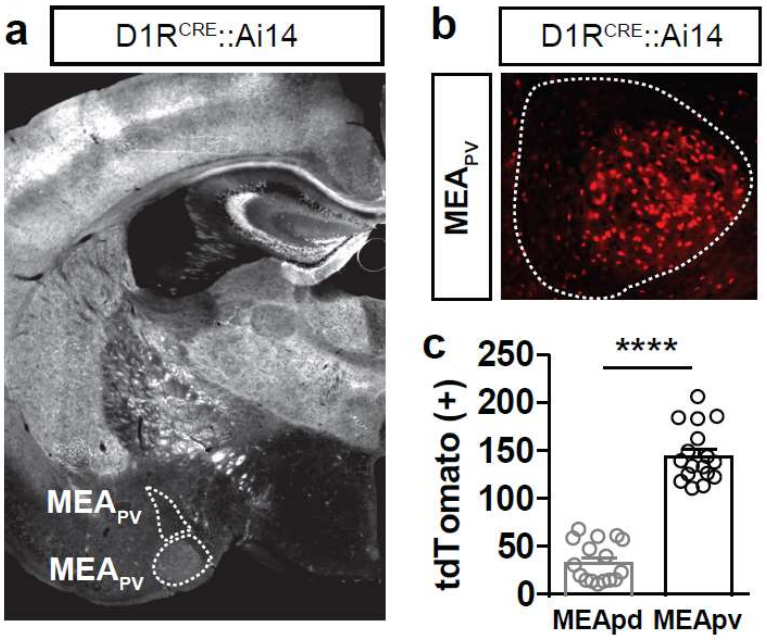

Figure 2: Identification of dopamine receptive neuron in the MEApv. (a) Coronal section of D1R$^{Cre/+}$::Ai14 reporter animal showing localization of tdTomato expressing *Drd1* neurons in the MEApv. (b) High-magnification image of D1R:tdTomato cells and (c) quantification showing increased expression of TdTmto-positive cells in MEApv versus MEApd (n=6-10 sections/animal, 2 animals/group, ****P<0.0001, unpaired *t* test).

Using cell-type specific expression of the stimulatory DREADD receptor hM3Dq in dopamine neurons of the ventral midbrain, we recently demonstrated that activation of dopamine neurons induces *c-fos* in the MEA[44]. To confirm the presence of dopamine receptive neurons in this region, we searched the Allen Institute for Brain Science Mouse Brain *in situ* hybridization atlas[45] for dopamine receptor expression in the amygdala. Within the MEA, *Drd1* was expressed prominently in the MEApv; high levels of *Drd1* were also observed in the intercalated cell clusters, and to a lesser extent in the BLA and CeA. In contrast, we did not observe appreciable levels of expression of *Drd2, 3, 4, or 5* in the MEA, though varying degrees of expression of these genes were seen in other amygdala nuclei. To confirm the presence of *Drd1*-expressing neurons in the MEA, we crossed *Drd1*$^{Cre/+}$ (D1R-Cre[46]) to the fluorescent reporter line Ai14[47]. Fluorescently labeled neurons were detected in the MEApv, and we observed a significantly higher number of tdTomato positive neurons in the MEApv as compared to the MEApd (Figure 2 a-c).

Expression relative to previously identified genes

We next wanted to confirm that *Drd1* was in fact a selective and specific marker

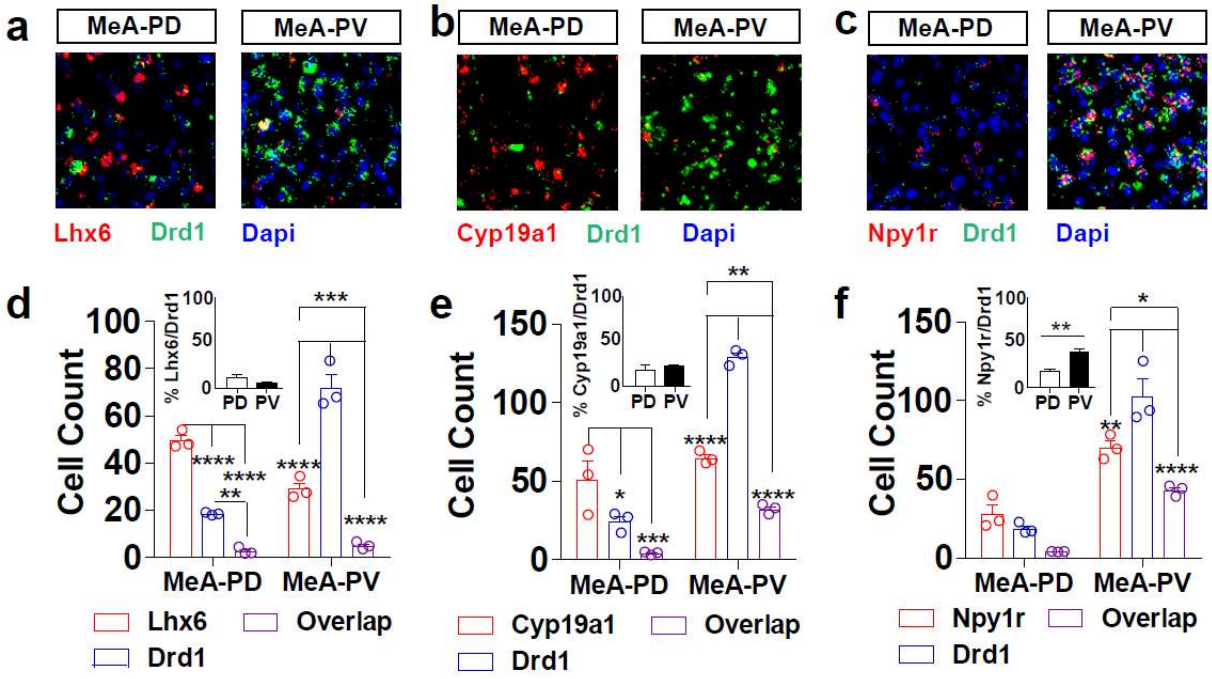

Figure 3: D1R specifically and selectively localizes to MEApv. (a) RNAscope ISH staining for Lhx6 vs. Drd1 (b) Cyp19a1 vs. Drd1 (c) Npy1r vs. Drd1. (d-f) Quantification comparing relative cell counts and overlap of puncta in 3 sections of MEAp (n=3 animals/gene).

of the MEApv relative to other genes that have previously been shown to localize within the MEA. Previous studies have used Lhx6, Cyp19a1 and NPYR1 as genetic markers of the MEApd, and we wanted to test whether Drd1 neurons represented a distinct population within the MEA. We employed RNAscope, a highly sensitive *in situ hybridization* assay that enables detection of target RNA in fixed tissue samples, to probe for the relative expression and co-expression of Drd1, Lhx6, Cyp19a1 and NYPR1. Due to particular experimental restrictions of RNAscope, we were only able to probe for two genes at one time. We found that across all experiments, Drd1 was more highly expressed in the MEApv relative to the MEApd, and relative to any other genes (Figure 3 a-c). Additionally, there was no significant overlap between Drd1 and any

other genes in either the MEApv or MEApd (Figure 3 a-c). These results support the conclusion that Drd1 is a specific and selective marker of the MEApv.

Dopaminergic innervation of MEApv

Consistent with innervation of the MEA by catecholamine producing neurons, immunohistochemistry for tyrosine hydroxylase (TH, the rate limiting enzyme in dopamine production) revealed TH-positive fibers in the MEApv (Figure 4a). Additionally, we injected the Cre-dependent, retrograde transducing virus CAV-FLEX-ZsGreen[16] into the MEApv of DAT-Cre mice and identified ZsGreen-positive dopamine neurons in the midbrain (Figure 4b). A direct projection from dopamine producing neurons of the ventral midbrain was confirmed by injection of a Cre-dependent adeno-associated virus (AAV1) containing an expression cassette for the fluorescent reporter synaptophysin-GFP (AAV1-FLEX-Syn-GFP[48][17] into the VTA/SNc of *Slc6a3*$^{Cre/+}$ (DAT-Cre[49]) mice (Figure 4c). Quantification of Syn-GFP puncta confirmed denser innervation of the MEApv compared to the MEApd (Figure 4d).

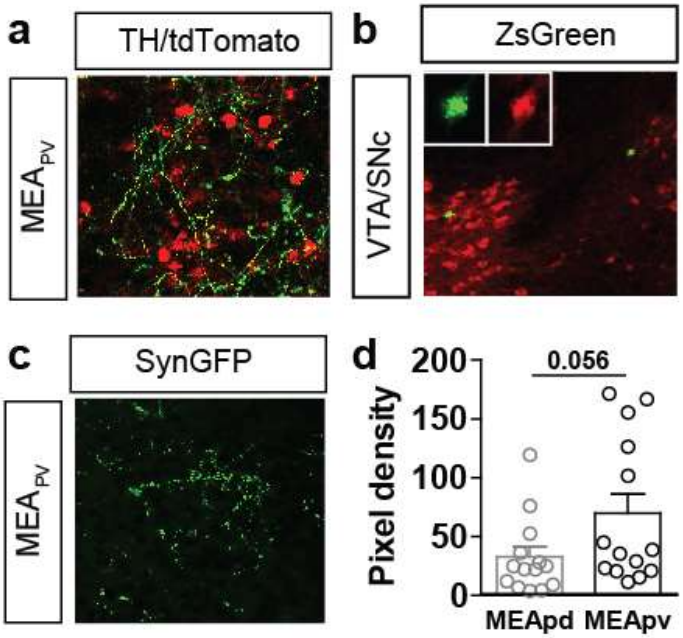

Figure 4: Dopamine fibers innervate MEApv. (a) Immunohistochemistry revealing tyrosine hydroxylase (TH) positive fibers in the MEApv. (b) Image showing retrogradely labeled CAV2-FLEX-ZsGreen expressing neurons co-localized with DAT(+) tdTomato expressing neurons in the midbrain.(c) Projections of midbrain DAT neurons revealed by expression of syn-GFP in axon terminals in the MEApv. (d). Quantification of projections showing denser projections to MEApv vs. MEApd (right) (n=6-8 sections/animal, 3 animals, P=0.056, unpaired *t* test).

To test for functional D1R signaling in the MEApv, we injected the D1R agonist SKF-81,297 intraperitoneally (7.5mg/kg) and immunostained for c-Fos protein. We

observed robust c-Fos in the MEA relative to saline controls, and higher c-Fos in the MEApv relative to the MEApd (Figure 5 a-b). Consistent with the excitatory nature of D1R activation, bath perfusion of SKF 81,297 (10μM) over acute brain slices during whole-cell patch clamp recordings increased the excitability of MEApv-D1R neurons following current injections (Figure 5 c-d). Approximately two-thirds of neurons showed increased action potential firing following SKF 81,297 application (Supplementary Figure 1a). Cells responsive to SKF 81,297 showed significantly higher action potential firing in response to current injection prior to SK 81,297 application (Supplementary Figure 1b), indicating higher baseline excitability. However, we did not observe differences in membrane potential prior to or following SKF 81,297 between responsive and non-responsive cells (Supplementary Figure 1c and d). Collectively, these data identify a population of dopamine-responsive neurons in the MEApv.

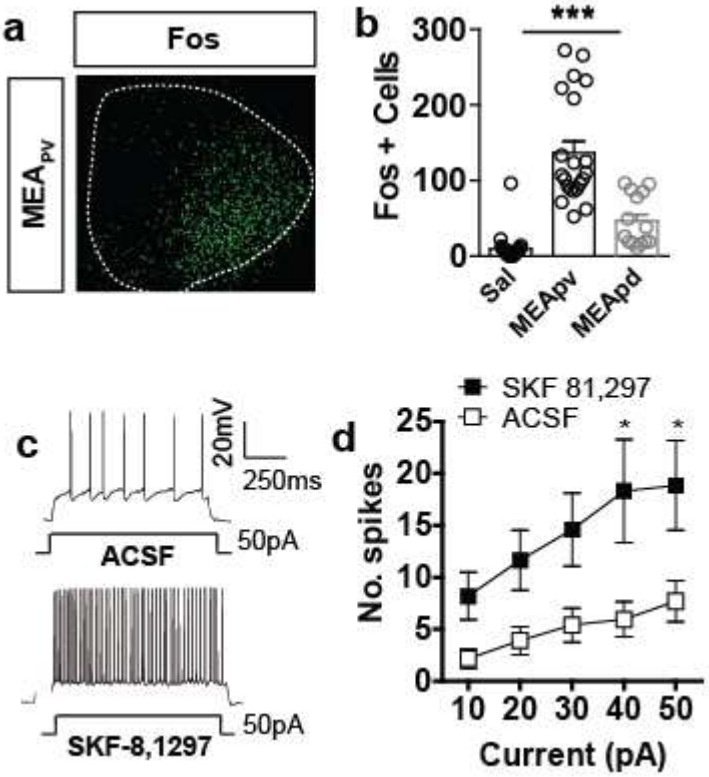

Figure 5: MEApv D1R neurons are functional. (h) Immunohistochemistry of MEApv following i.p. injection of SKF 81, 297 (7.5 mg/kg) showing increased FOS induction. (i) Quantification of Fos demonstrates a significantly higher *c-fos* induction in the MEApv compared to the MEApd (n=10-12 sections/animals, 3 animals/group, ****P<0.0001, unpaired *t* test). (j) Representative traces showing action potential firing before and after bath application of SKF 81,297 (10 μM). (k) Quantification of action potential firing shows increased MEApv-D1R spiking in response to current step injections following application of SKF 81,297 (n=20 cells/4 animals, *P<0.05, Bonferroni's multiple comparison test).

Chapter 3: MEApv-D1R neurons are activated by multiple innate threat stimuli

Introduction

Mounting evidence suggests an important role for the MEA in the mediation of approach and avoidance responses to threat stimuli, such as predator odorants and intruder conspecifics[13,18,50]. In particular, the MEApv has been implicated in these behavioral responses. For example, numerous studies have observed an increase in Fos activation in the MEApv compared to the MEApd when rodents are exposed to a predator or its odor, such as TMT[20]. In addition to threatening olfactory cues, other types of aversive stimuli have also been shown to activate the MEA. Rats exposed to an aversive tone[51] or air puff[52] show increased levels of Fos expression in the MEA. The MEA has also been implicated in social behaviors, particularly in approach and avoidance of threatening conspecifics[26]. During the resident-intruder assay, in which a subordinate mouse is placed into the home cage of a larger mouse, the resident animals show increased Fos activation in both the MEApv and MEApd[19,53]. Given that the MEApv is known to be activated by multi-sensory threat stimuli, we hypothesized that D1R neurons expressed in this region may also be involved in the processing of these types of stimuli.

Results

Activation of MEApv-D1R neurons in response to threat stimuli

To determine if MEApv-D1R neurons are specifically activated by innate threat stimuli, we virally labelled MEApv-D1R neurons with GFP and exposed animals to a

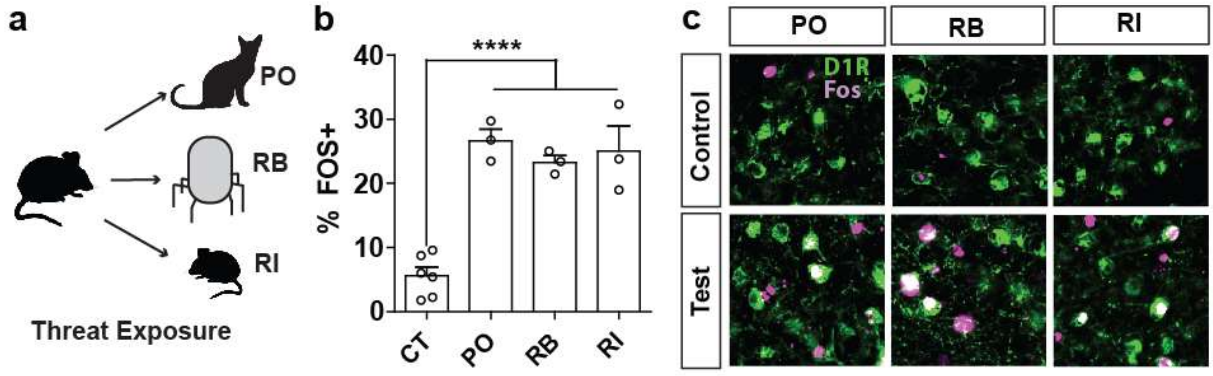

Figure 6: MEApv-D1R neurons are activated by multi-sensory threat stimuli. (a-c) Behavioral schematic, quantification and histological images of Fos levels in MEApv D1R neurons during exposure to threat stimuli. Fos is significantly induced in MEA$_{PV}$ D1R neurons over controls when animals are exposed to predator odor (PO), robobug (RB), and resident-intruder threat stimuli (RI) (n=8-10 sections/animal, 3 animals per group, 1-way ANOVA $F_{(3, 189)} = 55.05$, P<0.0001, ****P<0.0001, Bonferroni's multiple comparisons test).

variety of multi-sensory threats (Figure 6a). These threats included cat urine that evokes olfactory-based fear responses in mice[20] (predator odor, PO), an intruder conspecific that evokes olfactory, auditory, and visual social fear[18,26] (resident intruder, RI), and a robotic bug (robobug, RB) that simulates an auditory/visual predatory threat[50]. We observed increased Fos in a significant proportion of MEApv-D1R neurons in response to these cues that was equivalent across stimuli (Figure 6b and c; Supplementary Figure 2a and b).

In Vivo Ca^{2+} Imaging reveals neural representation of approach and avoidance during exposure to threat stimuli

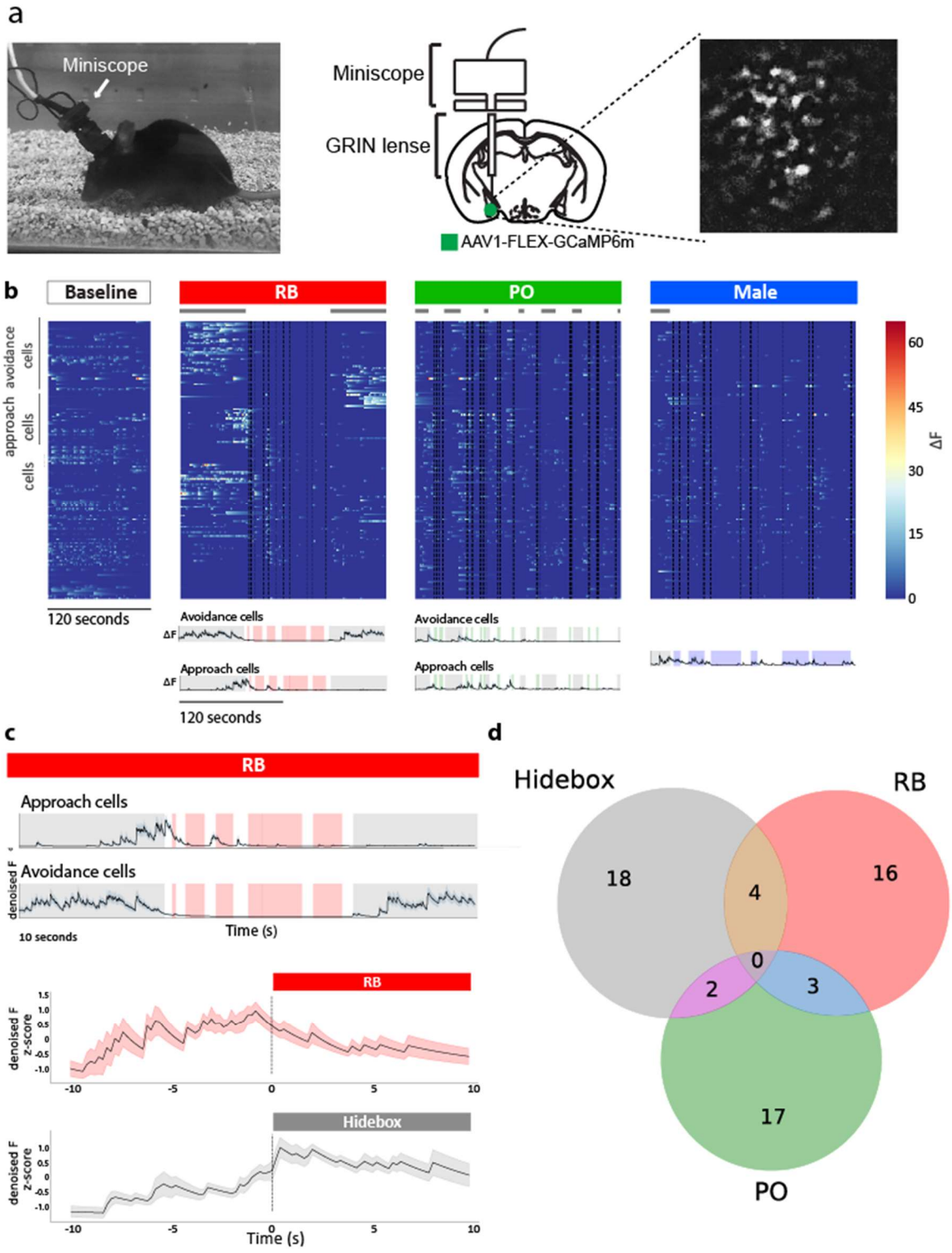

Figure 7: Calcium imaging reveals neural representation of approach and avoidance in MEApv. (a) Schematic showing behavioral and injection set up with FOV of cells for one animal. (b) Heatmap for one animal showing denoised fluorescent activity during behavioral paradigms. Gray boxes above indicate time animal spent in hidebox. Vertical black lines throughout indicate time animal was investigating the stimuli. Traces below each heatmap are an average of selective "approach" vs "avoidance" cells. (c) z-scores for for robobug period averaged across animals for neurons that increased in activity as animal approached RB and distinct population of neurons that sustained activity while animal was in hibebox. (d) representation of neuron selectivity across stimuli exposure. Numbers represent quantity of neurons active only during exposure to that stimulus. Numbers represent total across all animals. n=4 animals.

exposure to threat stimuli, we injected a conditional calcium indicator GCaMP6 into the MEApv of D1R-Cre mice. We implanted a gradient-index (GRIN) lens ~500um about the MEApv which was coupled to a head mounted Inscopix microscope while the animal freely explored an arena containing a threat stimulus (predator odorant or robobug) and hidebox. Cellular-resolution images images of MEApv-D1R neurons were captured live during behavior and analyzed using the open source CNMF-e script. During exposure to all stimuli, we observed MEApv-D1R neurons that were selectively active during periods in which the animal was approaching the stimulus ("approach" neurons). Furthermore, across all animals, "approach" neurons were selective for the stimulus, i.e, neurons active during approach to the robobug were distinct from neurons active during approach to the predator odorant. Interestingly, a separate population of MEApv-D1R neurons was active during periods in which animals were in the hidebox ("avoidance" neurons). These results imply that there is a heterogeneous population of D1R neurons in the MEApv that differentially encode approach and avoidance to distinct types of threat stimuli.

Chapter 4: Identification of anatomically and physiologically distinct MEApv-D1R circuits

Introduction

The afferent and efferent projections to and from the MEA are fairly well characterized. Notably, anatomical mapping studies have demonstrated that the MEA is densely innervated by all sensory cortices, particularly by the olfactory cortex[54]. The MEA has also been shown to send many important projections to brain regions involved in social and defensive behaviors such as the hypothalamus, the bed nucleus of the stria terminalis (BNST) and the periaqueductal grey (PAG)[22]. Additionally, these mapping studies reveal distinct projection patterns within discrete MEA nuclei. Importantly, the ventral and dorsal divisions of the MEA display particularly distinct patterns of efferent and afferent innervation[22]. Until recently, these anatomical mapping studies have not sufficiently addressed the cellular heterogeneity within the MEA. A recent study, however, investigated the electrophysiological properties and projections of specific cell types within the MEA. This study revealed that the MEApd contains a heterogeneous population of both non- GABAergic and GABAergic neurons, with a predominance of GABAergic neurons, all of which project to the hypothalamus[55]. While also heterogeneous, the majority of MEApv neurons were non-GABAergic. The study further identified a type of GABAergic neuron within the MEApv that forms local connections and provides feed-forward inhibition of sensory processing in the MEA[55]. Given this evidence, we hypothesized that MEApv-D1Rs may exhibit unique projection patterns and electrophysiological characteristics relevant to their functional properties.

Results

Anatomical mapping

Given that our calcium imaging results suggest that distinct populations of D1R neurons in the MEApv encode distinct types of defensive responses to threats, we hypothesized that were distinct circuits mediated by this population of neurons. To determine where MEApv neurons project, we bilaterally injected AAV-FLEX-Syn-GFP into the MEApv of D1R-Cre mice (Figure 8a). Consistent with previous reports of MEApv projections[22], we observed dense GFP-positive puncta in the VMHdm (Figure 8b) and transverse nucleus of the BNST (Figure 8c), with a bias toward a higher density projection to the BNST (integrated pixel density, BNST = 655.5 ± 105.4 versus VMH = 320.5 ± 105.9, P = 0.039, N = 3 mice). To determine whether projections from the MEApv to the VMH and BNST represent collaterals or independent projections, we co-injected retrogradely transported red fluorescent beads (RetroBeads) into the VMH and green RetroBeads into the BNST of wild-type mice (Figure 9a). Both red and green RetroBeads were observed in the MEApv, with a stronger labeling of BNST

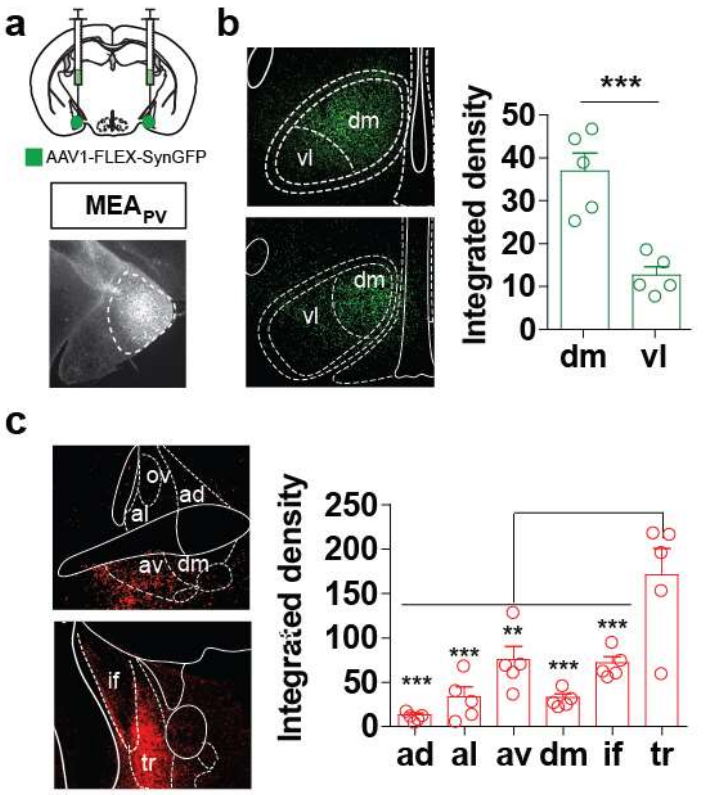

Figure 8: MEApv-D1R neurons project to distinct regions within VMH and BNST. (a) Schematic of bilateral viral injection of AAV1-FLEX-syn-GFP into MEApv of D1R$^{CRE/+}$ animal (adapted from[44]). Histology showing cell body expression of syn-GFP in MEApv D1R neurons, and revealing projections of MEApv D1R neurons in BNST and VMHdm.

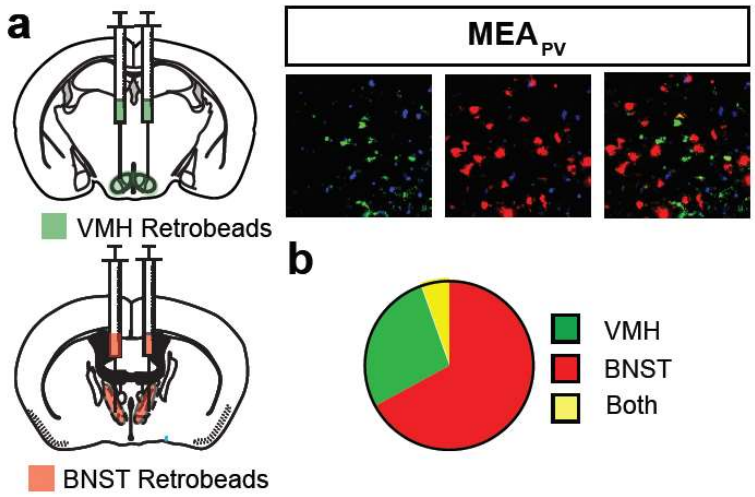

Figure 9: VMH and BNST-projecting MEA neurons are distinct within MEApv. (a) Schematic showing injection of green RetroBeads injected into the VMH and red RetroBeads injected into the BNST. (b)Significantly more MEA_{PV} neurons are labeled by BNST projections and there is very little overlap of green and red beads (70.9% red; 29% green; 5% overlap; n=8-10 slices/3 animals; P<0.0001, *Chi* squared).

projection neurons. Overall, we observed very few neurons with overlapping red and green fluorescent beads (Figure 9b).

Functional connectivity

To characterize the synaptic connectivity of MEApv-D1R neuron projections to the VMHdm and BNST, we transduced MEApv-D1R neurons with a conditional channelrhodopsin-2 (ChR2)-expressing virus (AAV1-FLEX-ChR2-mCherry). Following viral expression, we photostimulated MEApv-D1R terminals and performed whole-cell recordings in the VMHdm and the BNST (Figure 10 a - d). In the VMHdm, 9 out of 15 cells displayed a light-evoked excitatory postsynaptic current (EPSC) that was blocked by the AMPA glutamate receptor antagonist CNQX (Figure 10 c). We also observed one cell with delayed inhibition and one cell with delayed excitation, consistent with feedforward synaptic transmission. In the BNST, 15 out of 31 cells displayed a light-evoked inhibitory postsynaptic current (IPSC) that was blocked by the $GABA_A$ receptor antagonist picrotoxin (Figure 10 d). A smaller proportion of cells showed short latency excitation (3 of 31) or delayed inhibition (4 of 31) indicative of a smaller glutamatergic projection from the MEApv-D1R neurons. These data demonstrate a predominately excitatory MEApv

projection to the VMHdm and inhibitory projection to the BNST and are consistent with distinct populations of MEApv-D1R neurons projecting to the VMHdm or the BNST.

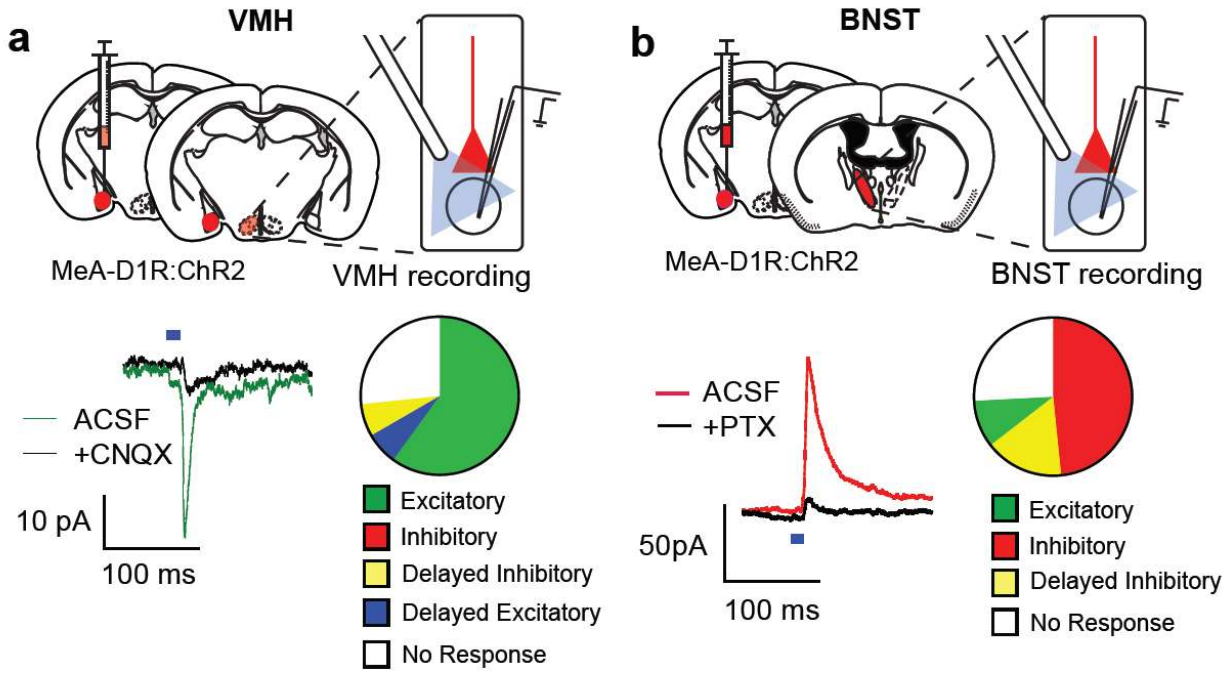

Figure 10: VMH and BNST-projecting MEApv-D1R neurons are physiologically distinct. (a) Schematic showing whole cell patch preparation in which ChR2-mCherry is transduced into the MEApv of $D1R^{CRE/+}$ mice and whole cell patch recordings are made in VMHdm. Example trace of blue light-evoked EPSC in the VMH_{DM} (holding at -60 mV); the EPSC could be blocked by bath application of CNQX (10 μM). Each trace is an average of 30 sweeps. Pie chart shows distribution of responses recorded in VMH. (b) Schematic showing whole cell patch preparation in which ChR2-mCherry is transduced into the MEApv of $D1R^{CRE/+}$ mice and whole cell patch recordings are made in BNST. Example trace of a blue light-evoked IPSC in the BNST (holding at 0 mV); the IPSC could be blocked by bath application of PTX (100 μM). Each trace is an average of 30 sweeps. Pie chart shows distribution of responses recorded in BNST.

Chapter 5: VMH and BNST-projecting MEApv-D1R neurons differentially regulate approach and avoidance to innate threat stimuli

Introduction

Both the VMH and BNST have been implicated in social and defensive behaviors. The VMH is dominantly involved in aggression and fear behaviors. Exposure to threatening conspecifics induces Fos in the ventrolateral VMH, and electro/opto-stimulation of this region evokes a robust aggression phenotype[23]. Electrical and optogenetic stimulation of the dorsomedial/central VMH elicits defensive behaviors such as freezing, hiding and increased heart rate[24]. The BNST is often studied as a node of anxiety[56], however it is also being increasingly appreciated for its role in defensive behavior. For example, exposure to the predator odor TMT induces robust Fos activity in the BNST[57,58], and muscimol-induced inactivation of the BNST blocks TMT-evoked freezing[59]. Taken together, these data support a hypothesis that VMH and BNST-projection MEApv-D1Rs may be involved the regulation of distinct domains of defensive behavior.

Results

Activation of VMH and BNST-projection MEApv neurons in response to threat stimuli

To determine whether BNST and VMH projecting MEApv neurons are differentially activated by threat stimuli, we injected RetroBeads into either the BNST or

VMH (Figure 11a) and exposed animals to predator odorant, robobug or the resident intruder assay. Consistent with our projection mapping, we observed a larger number of cells projecting to the BNST than to the VMH (Supplementary Figure 2c). BNST and

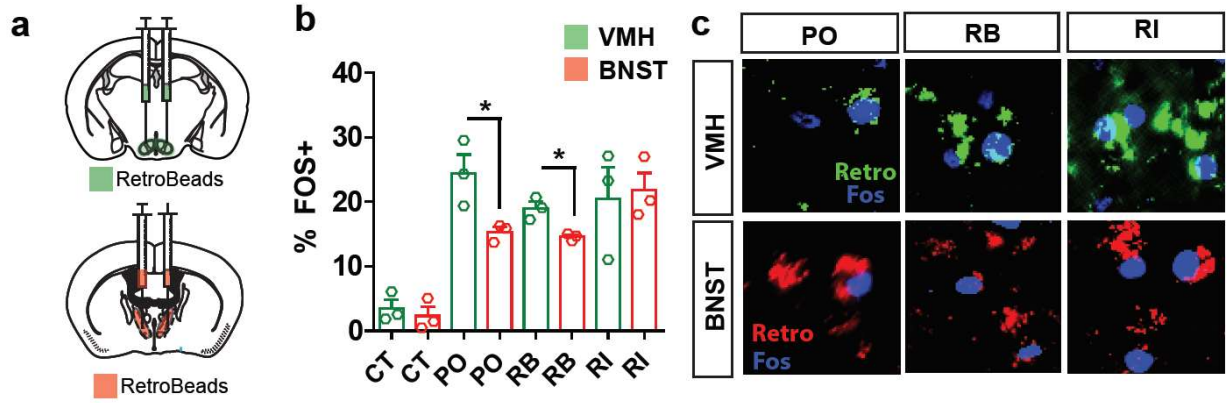

Figure 11: VMH and BNST-projecting MEApv neurons are activated by multi-sensory threat stimuli. (a-c) Injection schematic, quantification and histological images of Fos levels in VMH and BNST MEApv-projecting neurons during exposure to threat stimuli. There is significantly more Fos induction in VMH-projecting MEApv neurons compared with BNST-projecting MEApv neurons during predator odor and robobug exposure (P=0.002, *P=0.0134, unpaired *t* test).**

VMH projecting MEApv neurons were both activated by innate threat stimuli in all cases (Figure 11 b-c; Supplementary Figure 2d); however, a significantly larger proportion of VMH projecting MEApv neurons were activated by predator odor and robobug, but not to an intruder conspecific (Figure 11c).

VMH and BNST-projecting MEApv-D1R neurons are sufficient to regulate approach and avoidance behaviors

To determine the role of distinct MEApv-D1R circuits in innate defensive responses, we optogenetically stimulated MEApv-D1R→VMH and MEApv-D1R→BNST terminals (10Hz, 3 sec on/ 3 sec off) *in vivo* in the presence of innate threat stimuli (Figure 12a and b). MEApv-D1R neurons of $D1R^{Cre/+}$ mice were unilaterally transduced with AAV1-FLEX-ChR2-mCherry or AAV1-FLEX-mCherry (control), and an optic fiber

was implanted directly over the VMH or the BNST (Figure 12a; Supplementary Figure 3a-c).

Direct stimulation of MEApv-D1R→VMH projections enhanced defensive avoidance behaviors of a predator odor, resulting in increased time in the hide box (Figure 12c) and reduced time spent sniffing the odorant dish (Figure 12c). Latency to first approach of the predator odorant did not differ between groups (Supplementary Figure 4a), but the total number of approaches was reduced (Supplementary Figure 4a). In contrast to VMH stimulation, MEApv-D1R→BNST stimulation decreased avoidance of the predator odor, as measured by reduced time spent in the hide box (Figure 12c). We also observed an increase in approach of the stimulus as measured by an increase in approach frequency and an increase in sniffing time when compared to MEApv-D1R→VMH stimulation (Supplementary Figure 4a, Figure 12c).
Similar to the behavioral response to predator odor, we observed opposing behavioral responses to the robobug. Stimulation of the MEApv-D1R→VMH pathway increased and stimulation of the MEApv-D1R→BNST pathway decreased time in the hidebox (Figure 12d). Opposing effects were also observed on latency to reinvestigate following the initial flight caused by activation of robobug movement and total investigation time (Figure 12d, Supplementary Figure 4b). In response to both the predator odor and robobug, stimulation of BNST terminals resulted in an active approach and exploration of these stimuli.

In response to a conspecific threat, male mice will display territorial aggression towards an intruder[60]. To assess whether MEApv-D1R projections to the VMH or BNST influence this behavior, we stimulated these projections during a resident-intruder

assay[26]. We observed distinct defensive behaviors between the MEApv-D1R→VMH and MEApv-D1R→BNST stimulated mice. MEApv-D1R→VMH stimulated mice showed significantly increased grooming of the male conspecific intruder and less aggression (Figure 12e). MEApv-D1R→BNST stimulated mice showed a slight reduction in grooming of the male conspecific intruder and a significantly increased aggression phenotype (Figure 12e). We did not observe significant differences in total investigation time across the groups). These data demonstrate that grooming and aggression towards conspecifics are bi-directionally controlled by distinct MEApv circuits.

To establish whether MEApv-D1R→VMH or MEApv-D1R→BNST connections are inherently rewarding or aversive, we performed a real-time place preference (RTPP) assay[61] during terminal stimulation. We observed an increased avoidance of the light-paired chamber in MEApv-D1R→VMH stimulated mice relative to the unpaired side (Figure 12f). In contrast, MEApv-D1R→BNST stimulation had no significant effect on RTPP behavior (Figure 12f). This suggests that the increased exploratory behavior observed in response to the other threat assays is likely specific for discrete sensory stimuli. We also observed a significant difference between MEApv-D1R→VMH and MEApv-D1R→BNST stimulation on total distance travelled during the RTPP assay, with the MEApv-D1R→VMH group showing less locomotion than the MEApv-D1R→BNST group; however, neither differed significantly from controls (Figure 12f).

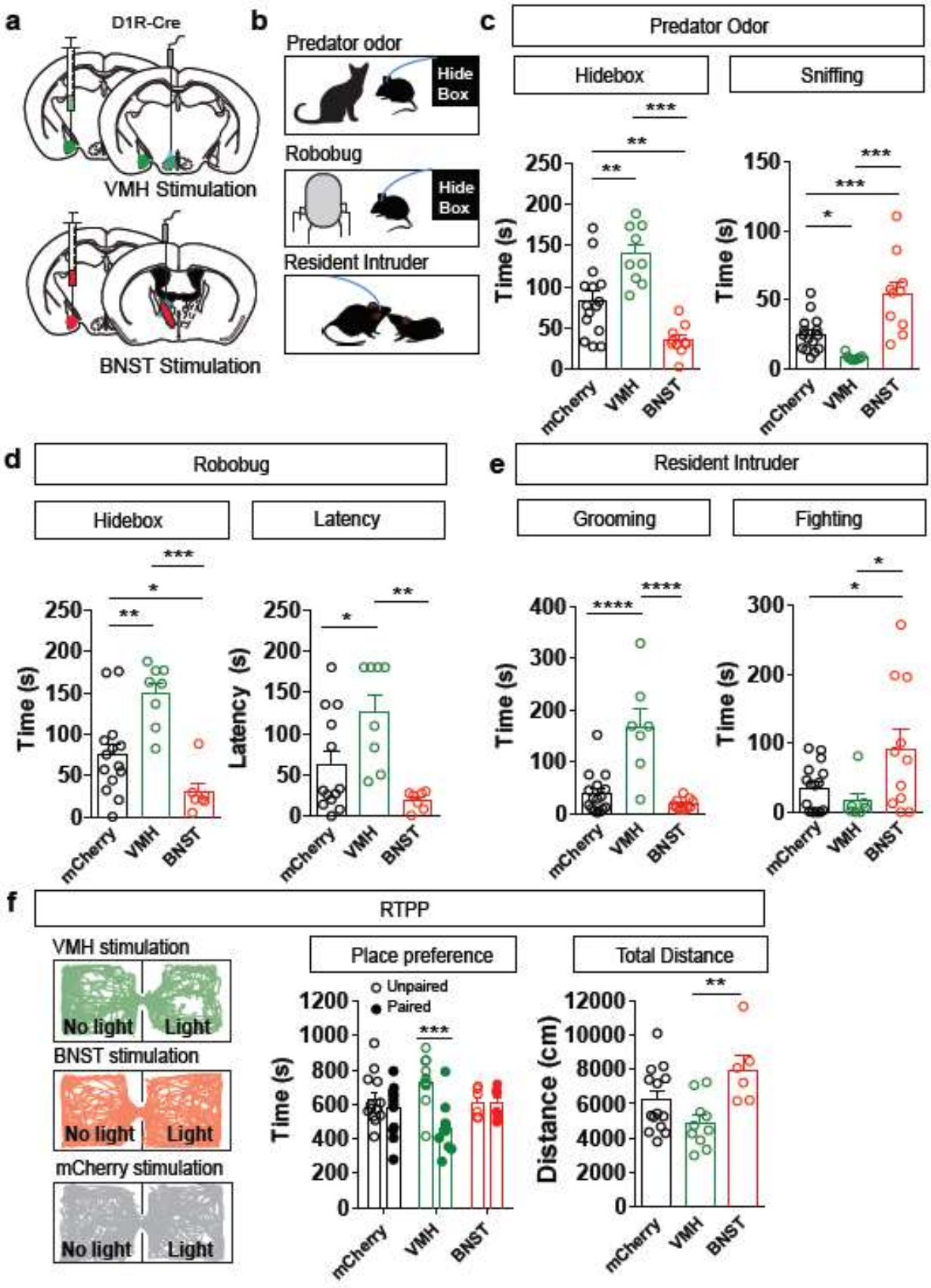
a
D1R-Cre
VMH Stimulation
BNST Stimulation
b
Predator odor
Hide Box
Robobug
Hide Box
Resident Intruder
c
Predator Odor
Hidebox
Sniffing
Time (s)
mCherry
VMH
BNST
d
Robobug
Hidebox
Latency
Time (s)
Latency (s)
e
Resident Intruder
Grooming
Fighting
Time (s)
f
RTPP
VMH stimulation
No light
Light
BNST stimulation
mCherry stimulation
Place preference
Unpaired
Paired
Time (s)
Total Distance
Distance (cm)

Figure 12: VMH and BNST-projecting MEApv-D1R neurons differentially regulate innate fear. (a-b) Schematic of viral injection of AAV1-FLEX-ChR2-mCherry, fiber-optic implant, and behavioral paradigms for threat exposure. (c) Optogenetic activation of VMH-projecting MEApv- D1R neurons increases time spent in hidebox during exposure to predator odorant and decrease sniffing of the odorant container. Optogenetic activation of BNST-projecting MEApv D1R neurons decreases time spent in hidebox during exposure to predator odorant and increases sniffing of the odorant container (n=9-10 animals/group; 1-way ANOVA $F_{(2, 31)} = 20.39$, P<0.0001, Tukey's multiple comparisons test **P<0.01, ***P<0.001). (d) Optogenetic activation of VMH-projecting MEApv- D1R neurons increases time spent in hidebox and increases latency to re-investigate an activated robobug. Optogenetic activation of BNST-projecting MEApv D1R neurons decreases time spent in hidebox and decreases latency to re-investigate an activated robobug (n=6-8 animals/group; 1-way ANOVA $F_{(2, 26)}= 15.19$, P<0.0001; Bonferroni's multiple comparisons test *P<0.05, **P<0.01, ***P<0.001). (e) Optogenetic activation of VMH-projecting MEApv- D1R neurons increases grooming of conspecific during resident intruder assay and optogenetic activation of BNST-projecting MEApv D1R neurons increases fighting of conspecific during resident intruder assay (grooming: n=7-11 animals/group; 1-way ANOVA $F_{(2, 31)}= 21.34$, P<0.0001; Bonferroni's multiple comparisons test ****P<0.0001; fighting: n=7-11 animals/group; 1-way ANOVA $F_{(2, 31)}= 4.297$, P=0.02251; Bonferroni's multiple comparisons test *P<0.05). (f) Representative real time place preference (RTPP) location plots (left). Quantification of RTPP (right) shows that optogenetic activation of VMH-projecting MEApv D1R neurons reduces time spent in light paired chamber, but activation of BNST-projecting MEApv D1R neurons has no effect (2-way ANOVA $F_{(2, 29)} = 3.31$, P=0.05; ***P<0.001 Bonferroni's multiple comparisons). Total distance traveled was reduced in VMH stimulated versus BNST stimulated MEApv-D1R terminals in the RTPP assay (1-way ANOVA $F_{(2, 29)} = 5.766$, P=0.0082; **P<0.01 Tukey's multiple comparison test)

VMH and BNST-projecting MEApv-D1R neurons are necessary to regulate approach and avoidance behaviors

To determine the necessity of distinct MEApv-D1R circuits in innate defensive responses, we optogenetically inhibited MEApv-D1R→VMH and MEApv-D1R→BNST terminals (2 secs off, 1 second ramp down) *in vivo* in the presence of innate threat stimuli. MEApv-D1R neurons of $D1R^{Cre/+}$ mice were bilaterally transduced with a conditional retrogradely traveling AAV2 virus expressing Jaws, a red-shifted chloride pump, injected into either the BNST or VMH, and an optic fiber was implanted directly over the MEApv (Figure 13a).

In contrast to stimulation, inhibition of MEApv-D1R→VMH projections robustly increased approach to a predator odor, which was observed as increased time spent investigating the odorant and reduced time spent in the hidebox (Figure 13b). Conversely, MEApv-D1R→BNST inhibition increased avoidance of the predator odor, as measured by increased time spent in the hide box (Figure 13b). Similar to the behavioral response to predator odor, we observed opposing behavioral responses to the robobug. Inhibition of the MEApv-D1R→VMH pathway reduced and inhibition of the MEApv-D1R→BNST pathway increased time in the hidebox (Figure 13c). In response to both the predator odor and robobug, inhibition of VMH terminals resulted in an active approach and exploration of these stimuli.

Next, we inhibited MEApv-D1R projections to the VMH or BNST these projections to assess whether their necessity in territorial aggression as a measure of

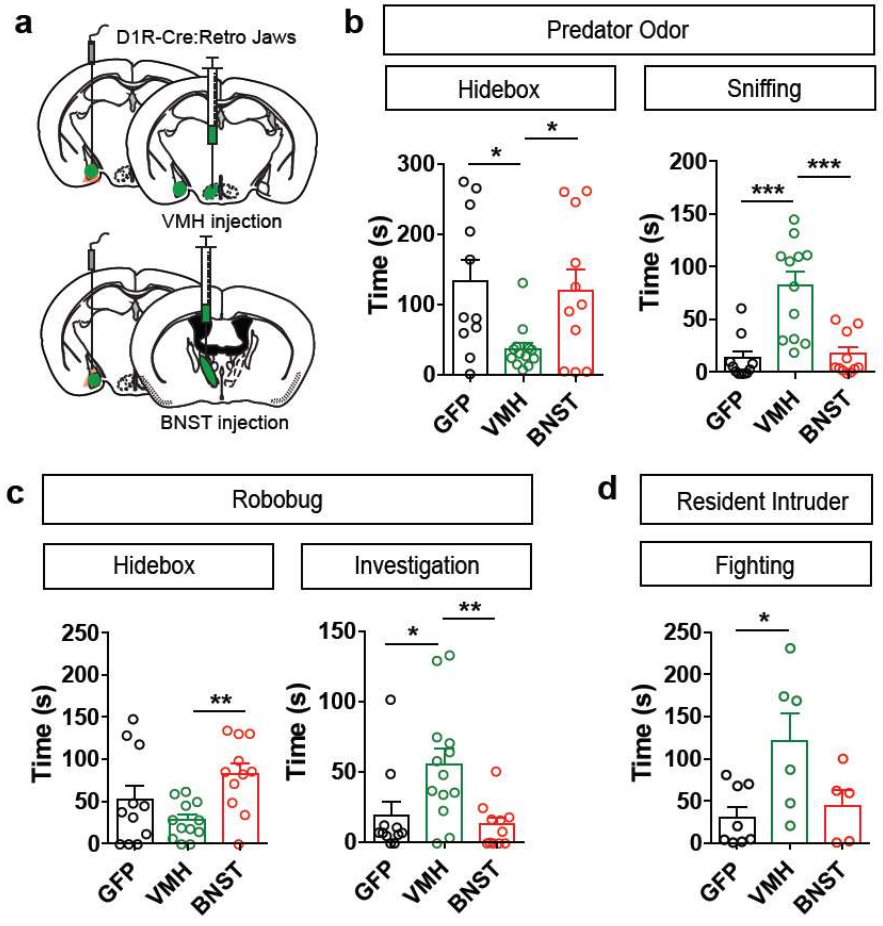

Figure 13: Inhibition of VMH and BNST-projecting MEApv-D1Rs bidirectionally modulates approach and avoidance

approach and avoidance toward a conspecific threat. Similar to stimulation, we observed distinct differences in defensive behaviors between the MEApv-D1R→VMH and MEApv-D1R→BNST inhibited mice. Inhibition of MEApv-D1R→VMH terminal evoked a robust aggression phenotype, whereas inhibition MEApv-D1R→BNST projections did not generate any observable behavioral phenotype (Figure 13d). We did not observe significant differences in total investigation time across the groups (Supplementary X). These data reinforce our findings that grooming and aggression towards conspecifics are bi-directionally controlled by distinct MEApv circuits.

To establish whether MEApv-D1R→VMH or MEApv-D1R→BNST connections are inherently rewarding or aversive, we implemented the RTPP assay during terminal inhibition to further assess whether MEApv-D1R→VMH or MEApv-D1R→BNST connections are necessarily inherently rewarding or aversive. We observed a slight increase in avoidance of the light-paired chamber in MEApv-D1R→BNST inhibited mice relative to the unpaired side (Figure tbd). In contrast, MEApv-D1R→VMH inhibition had no significant effect on RTPP behavior (Figure tbd). This reinforces our hypothesis that discrete sensory stimuli elicit exploratory behavior.

Chapter 6: Dopaminergic modulation of approach and avoidance within MEApv circuit

Introduction

When confronted with a threat, an organism depends on selecting an appropriate behavioral response in order to survive. Within complex environments, organisms require sophisticated mechanisms to flexibly make decisions about whether to approach or avoid a threat based on its perceived risk or reward. Recent studies have provided evidence for circuit mechanisms enabling rapid and adaptive action selection in the face of threats. There are distinct and mutually inhibitory neurons in the central amygdala that regulate the selection between active (escape) and passive (freezing) fear responses[62]. Additionally, distinct populations of interneurons within the laterodorsal tegmentum (LDT) bi-directionally regulate innate fear responses to a predator odor, underlying a mechanism for scalable behavior responses[63]. Finally, GABAergic neurons in the MEA gate social behaviors, specifically fighting, through an intensity coding mechanism revealed through scaling the power of optogenetic stimulation during a social interaction test[26]. This suggests a cellular mechanism by which neural circuits might encode scalable decision making. For example, neuromodulators may differentially act on a population of neurons depending on their activation threshold. Taken together, these data begin to reveal a circuit organization by which animals might make rapid decisions between competing behaviors when faced with conflicting cues. Our connectivity analysis indicates that MEApv-D1R neurons are heterogeneous, and dominantly release glutamate at VMHdm terminals and GABA at BNST terminals. We also demonstrate that these circuit connections regulate innate defensive behaviors in

opposite directions. We hypothesized that this may be another circuit mechanism

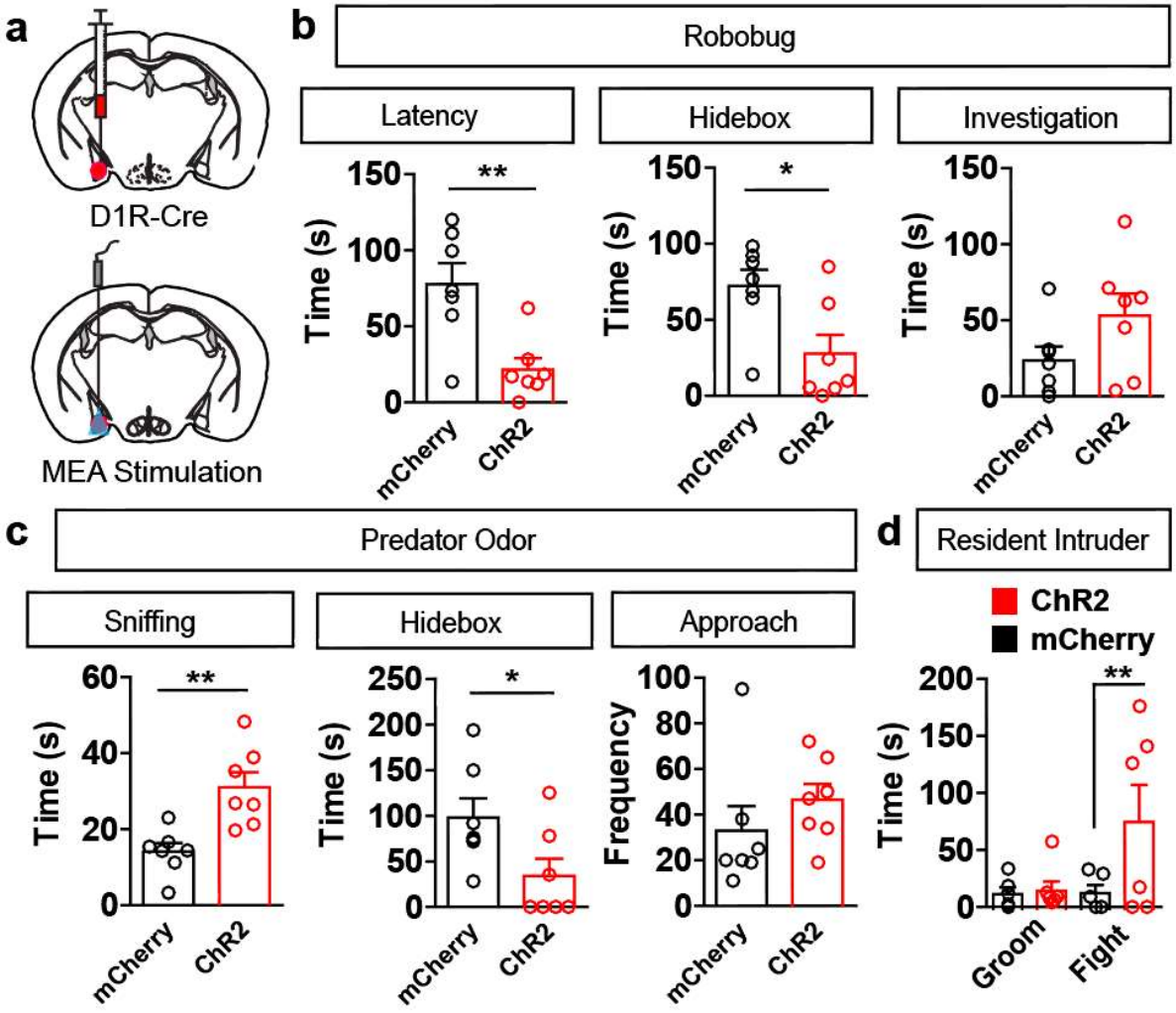

underlying flexible decision making in the face of threat and was likely modulated by

Figure 14:) Schematic of viral injection of AAV1-FLEX-ChR2-mCherry and optic fiber implant into MEApv of D1R$^{Cre/+}$ mice. (b) Optogenetic activation MEApv-D1R neurons increases approach to robobug as evidenced by significantly reduced latency to investigate robobug (n=7 animals/group; **P = 0.0038, unpaired *t* test) and significantly reduced time in hidebox during robobug exposure (*P = 0.0186, unpaired *t* test). Total investigation time was not altered (P = 0.11). (c) During exposure to predator odor, optogenetic activation of MEA$_{PV}$-D1R neurons results in significantly more time sniffing predator odor (n= 7 animals/group; **P = 0.0027, unpaired *t* test) and less time in hidebox during exposure to predator odor (*P = 0.0431, unpaired *t* test) . Frequency of approach as not significantly affected (P = 0.3131, unpaired *t* test). (d) Optogenetic activation of MEA$_{PV}$-D1R neurons increases fighting during resident intruder assay, but does not influence grooming behavior (n= 5-6 animals/group; **P=0.0091, unpaired *t* test).

dopamine.

Results

Global activation of MEApv-D1R neurons biases approach over avoidance

To determine whether these circuits are truly diametrically opposed, or whether one of these distinct circuits can dominate the other, we optogenetically stimulated MEApv-D1R cell bodies (Figure 14a) in the presence of innate threat stimuli. Like MEApv-D1R→BNST terminal stimulation, collective stimulation of MEApv-D1R cell bodies reduced fear in the predator odor and robobug assay, and enhanced aggression in the resident-intruder assay (Figure 14b-d, Supplementary Figure 5a and b). MEApv-D1R cell body stimulation did not induce a change in behavior in the RTPP assay (Supplemental Figure 5c) and was not associated with changes in locomotion (Supplemental Figure 5c). These data are in agreement with our tracing data showing a more dominant projection to the BNST and suggests that when co-activated, the BNST pathway overrides the VMH circuit to bias behavior towards approach.

Infusion of DA agonist into MEApv biases approach over avoidance

It is well established that transient elevated levels of dopamine release in the

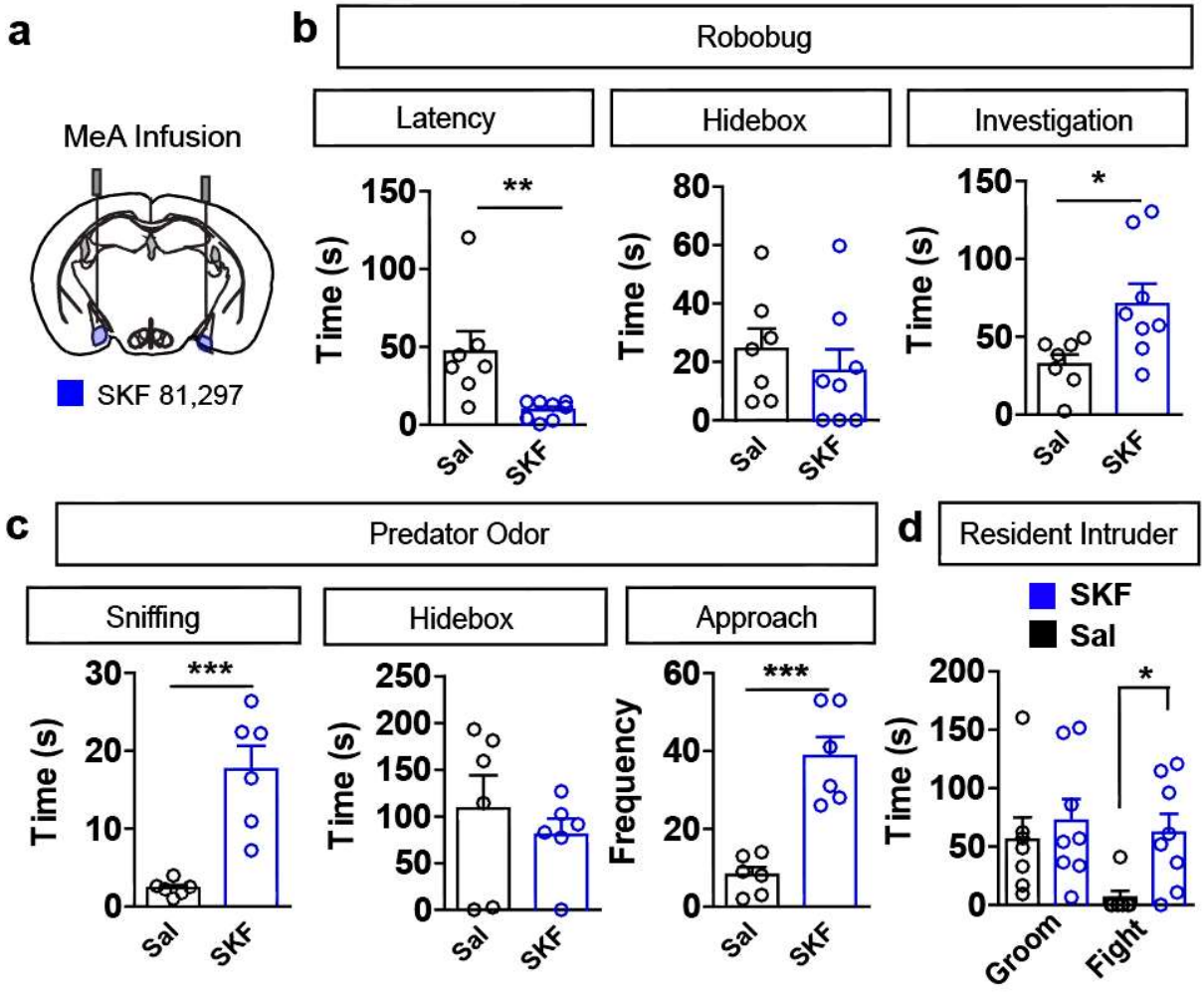

Figure 15(a) Schematic of bilateral microinfusion of D1R agonist SKF 81, 297 (3µg/0.5µl per side) locally into the MEA. (b) Infusion of SKF reduced latency to investigate robobug (n=7-8 animals/group; *P = 0.0101, unpaired *t* test) and increased investigation of robobug (*P = 0.0249, unpaired *t* test), but did not alter time in hidebox (P = 0.4751, unpaired *t* test). (c) Infusion of SKF 81,297 increased sniffing of odorant container (n= 6 animals/group; ***P=0.0005, unpaired *t* test) and s increased frequency of approaches to odorant container (*P = 0.0002, unpaired *t* test), but did not alter time in hidebox (P = 0.4912, unpaired *t* test). (d) Infusion of SKF 81,297 increases fighting during resident intruder assay but has no effect on grooming behavior (n = 7-8 animals/group; $F_{(3, 26)} = 3.161$, *P=0.0414, 1-way ANOVA, Bonferroni's multiple comparisons test, *P<0.05).**

striatum promote conditioned approach to rewarding stimuli that is mediated in part by dopamine signaling through D1R[28] to enhance incentive motivational drive[29]. To determine whether increasing dopamine D1R signaling on MEApv-D1R neurons biases behavior similarly to optogenetic stimulation of this pathway, we bilaterally infused the

D1R agonist SKF 81,297(3µg/0.5µl per side) directly into the MEApv of wild type mice through stereotaxically implanted cannula (Figure 15a). Like MEApv-D1R optical stimulation, infusion of SKF 81,297 suppressed fear responses following exposure to innate threat stimuli and enhanced approach and aggression (Figure 15b-c and Supplementary Figure 5d and e). SKF 81,297 infusion did not alter locomotor behavior in these assays (Supplementary Figure 5f). Taken together, these data support a role for MePV-D1R neurons in the modulation of innate fear behavior and demonstrate that the MEA-D1R→VMH and MEA-D1R→BNST pathways are not equivalent in their opposition, but rather can be biased toward approach when globally activated. We propose that during periods of high incentive motivation, such as during the drive to acquire rewards, behavior is biased towards approach in the face of potential danger that is predicated by state-dependent levels of dopamine in the amygdala.

DA agonist differentially activates VMH vs. BNST projecting MEApv-D1R neurons

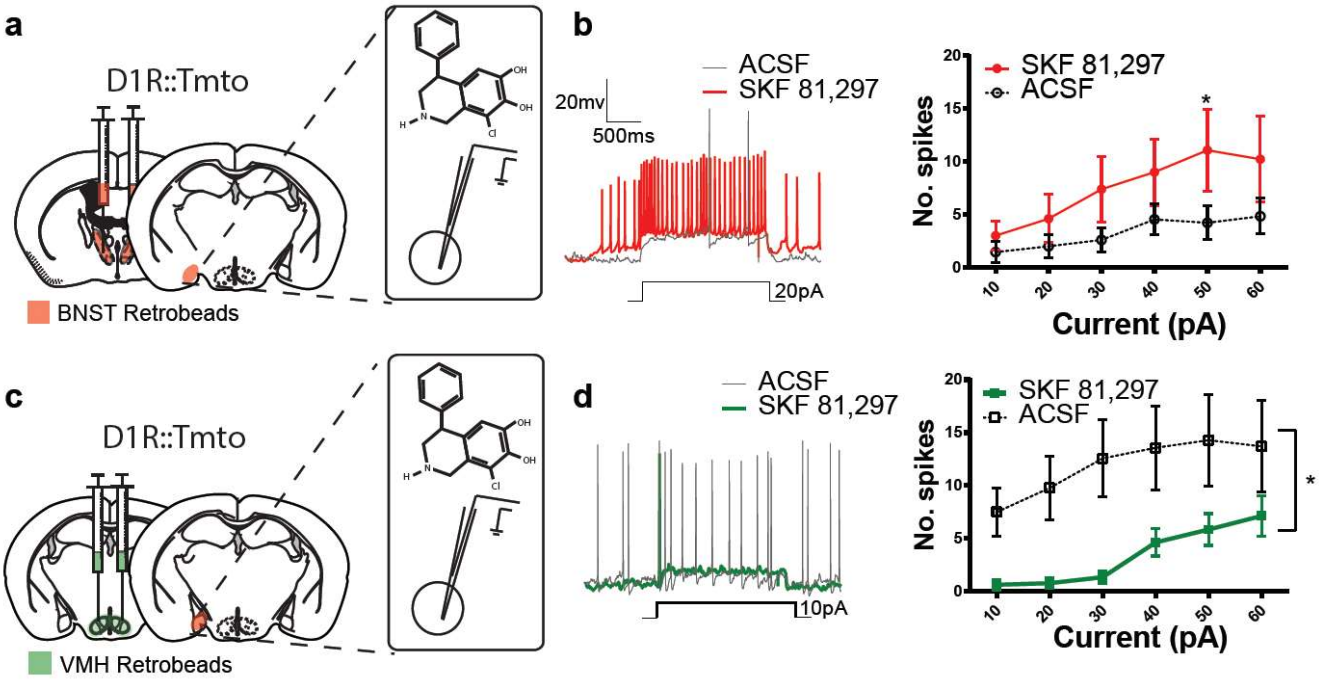

Figure 16: Dopamine agonist paradoxically inhibits VMH-projecting MEApv-D1R neurons.

Given that the binding properties of DA receptors can change in response to fluctuations in synaptic physiology, and in particular, D1R activation is observed to have inhibitory effects, we hypothesized that the VMH and BNST-projecting MEApv-D1R neurons may be differentially activated by dopamine. In order to test this, we used *in vitro* slice electrophysiology to look at evoked action potentials in VMH vs. BNST-projecting MEApv-D1R neurons. We injected green Retrobeads into either the VMH or BNST of *Drd1*$^{Cre/+}$;Ai14 mouse to selectively label VMH or BNST projecting Tmto-labeled D1R neurons in the MEApv (Figure 16a, c). Consistent with the excitatory nature of D1R activation, bath perfusion of SKF 81,297 (10μM) over acute brain slices during whole-cell patch clamp recordings increased the excitability of BNST-projecting MEApv-D1R neurons following current injections (Figure 16b). Interestingly, VMH-projecting MEApv-D1R neurons were spontaneously active at baseline and exhibited a paradoxical inhibition of action potential firing following current injections (Figure 16d).

This suggests an alternative mechanism by which D1 receptors signal in VMH vs. BNST-projecting MEApv neurons. There is an increasing body of evidence supporting differential coupling mechanisms of D1Rs in striatal and amygdalar neurons (see Ch.1 introduction). We hypothesize that these differential effects of dopamine provide a cellular mechanism by which VMH and BNST projections from the MEApv flexibly regulate approach and avoidance behavior.

Chapter 7: Discussion and Future Directions

Organisms across all levels of complexity possess approach mechanisms, which

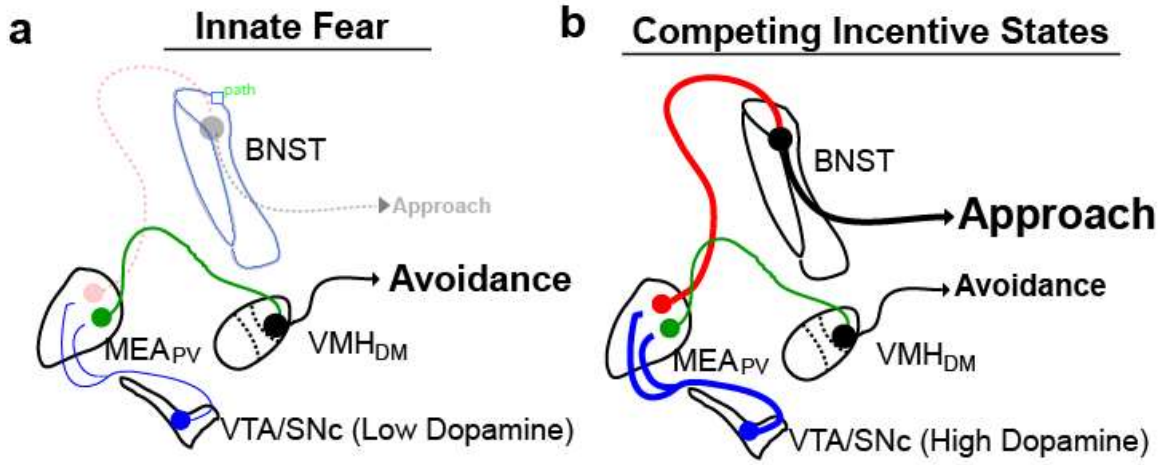

Figure 17: Proposed model for how competing incentive states modulate VMH versus BNST MEA$_{PV}$-D1R pathways depending on dopamine levels in the amygdala. (a) Under low competing incentive states when dopamine levels are low the MEApv-D1R→ VMH pathway predominates to mediate avoidance. (b) Under high competing incentive states when dopamine levels are increased the MEApv-D1R→BNST predominates to mediate approach in the face of danger.

evoke social and explorative behavior, and avoidance behaviors, which evoke withdrawal and flight[1]. In order to maximize gains, animals will engage in risky exploratory behavior, ignoring signs of potential threat, to exploit resources in their environment. Animals exposed to competing environmental cues must negotiate between mutually incompatible behaviors, such as feeding, reproduction, flight or defense. In some contexts, threatening stimuli, such as predators or aggressive conspecifics, will suppress appetitive behavior, such as reproduction[21]. Conversely, hunger and food seeking will override defensive behaviors[30]. Additional evidence suggests that defensive responses can be adaptive depending on the fed state of an animal and that these adaptations specifically involve neurons in the MEApd[64]. Thus, animals require integrated circuits to generate gradients of defensive responses appropriate to the contextual threat, and approach responses proportional to potential gains.

We find that MEApv-D1R neurons can be parsed into their inhibitory and excitatory projections to the BNST and VMH, respectively, to differentially regulate defensive behavior. MEApv-D1R neurons that evoke GABA-mediated inhibition of the BNST elicit approach behavior to threat stimuli, including aggression towards conspecifics. Our observations echo previous work showing that inactivation of the BNST suppresses innate fear behavior in response to predator odors[59]. Conversely, MEApv-D1R neurons that evoke glutamatergic excitation of the VMHdm enhance avoidance of threatening stimuli and grooming of conspecifics. Consistent with our observation, stimulation of the VMHdm enhances innate fear behaviors such as hiding and freezing[65]. Thus, the dopamine-modulated circuit organization described here provides a mechanism by which conflicting motivational systems interact to generate biased responses. We propose that basic approach and avoidance behaviors are encoded through amygdalar-hypothalamic circuits in a scalable manner depending on physiological levels of dopamine present in the MEApv (Figure 17 a-b). For example, during periods when dopamine levels are high and induced by some physiological need of the organism, MEApv biases approach behavior over avoidance in threatening situations (Figure 17b). Further studies are needed to investigate the physiological function of dopamine in this circuit.

The amygdala is composed of multiple distinct and interconnected nuclei involved in threat detection[18], as well as hedonic and consummatory processes[66,67]. The MEApd and MEApv are thought to be differentially involved in defensive responses to either conspecifics or predators[18,19]. In rodents, the MEApd is robustly activated by aggressive conspecifics, while the MEApv is strongly activated by

a live cat or its odor[19-21,68,69]. Anterograde tracing studies have demonstrated that the MEApd projects to regions implicated in reproduction and conspecific responsive behavior, including the ventrolateral VMH (VMHvl)[22,23]. In contrast, the MEApv projects to distinct hypothalamic nuclei involved in predator-responsive and general avoidance behavior, including the VMHdm[22,24]. Activation of independent pathways from the VMHdm to either the periaqueductal gray or the anterior hypothalamic nucleus can evoke either freezing or avoidance in response to threats, respectively[24]. Both subdivisions of the MEA project densely to the BNST, a region involved in both unconditioned fear responses to a predator odorant[59] and conspecific male aggression[64].

Based on previous hypotheses that conspecific and predatory threats are differentially regulated by the MEApd and MEApv[65,70], respectively, we were surprised to find that projection-specific pathways from the MEApv differentially regulated conspecific male aggression. However, our data are consistent with previous reports showing *c-fos* induction in the MEApv in response to male conspecific[23]. This raises the interesting point*, is conspecific male aggression defensive or appetitive?* Aggressive behavior towards intruder conspecifics was once viewed as a purely defensive response; however, recent studies have revealed that aggression in rodents generates a conditioned place preference and increases nucleus accumbens dopamine levels[71,72]. Specifically, microdialysis experiments in the nucleus accumbens in aggressive males revealed that DA levels increase prior to an anticipated fight and can remain elevated during and after a single fight[72]. Additionally, local dopamine receptor blockade in the nucleus accumbens decreases aggression motivated operant responding[73]. Importantly,

our findings that activation of the MEApv-D1R→BNST pathway increases aggression may reflect a parallel or integrated mechanism by which increased amygdalar dopamine generates a motivational state to drive aggression.

Dopamine has been implicated as central to incentive motivational processes underlying reward seeking and conditioned fear, but whether dopamine is a key modulator of circuits underlying approach and avoidance conflict has not been established. Here we demonstrate a role for dopamine in innate fear behavior through the modulation of dopamine D1R signaling in the MEApv. Specifically, we show that increasing D1R signaling onto MEApv-D1R neurons, as well as co-activation of MEApv-D1R→BNST and MEApv-D1R→VMH pathways, biases approach behavior. These data suggest that dopamine levels in the MEApv modulate the enhancement or suppression of defensive responses. Based on electrophysiological recordings, fast-scan cyclic voltammetry, and microdialysis during appetitive and aversive behaviors, it has been proposed that dopamine can differently modulate behavior based on the timescale of release, with transient phasic dopamine enhancing rewarding motivating processes and slow-sustained dopamine release regulating aversive outcomes[74]. Therefore, we propose that under threat conditions, low levels of dopamine promote activation of an avoidance-selective pathway in the MEApv that overrides innate approach behavior. In contrast, when dopamine levels are high, such as during reward seeking under threatening conditions, the avoidance-selective pathway is overridden by the MEApv approach pathway. Interestingly, it has recently been shown that activation of distinct inhibitory subpopulations within the laterodorsal tegmentum (LDT) oppositely regulate olfactory cue-induced freezing to an innate threat[63]. Given that the LDT is a potent

regulator of the midbrain dopamine system this represents a putative mechanism for differential regulation of MEApv dopamine levels through inhibitory/disinhibitory circuits of the LDT.

Future Directions

This work has identified a potential role for dopamine in the modulation of basic approach and avoidance behaviors through a unique amygdalar-hypothalamic circuit. Further electrophysiological studies are needed in order to better understand the mechanism by which D1R is differentially acting on VMH vs BNST-project MEApv-D1R neurons. We propose to supplement the current experiments presented here with additional studies looking at the role at resting state membrane potential, as well as GIRK channels, in the effects of inhibition of D1R activation in VMH-projecting neurons. Additionally, a better understanding of how dopamine functions physiologically in this circuit requires further investigation. We propose that during exposure to a threat, high and low levels of dopamine in the MEA bias activation of either the BNST or VMH circuit, and determine the appropriate behavioral response. In order to test the physiological basis of this hypothesis, we suggest tests the role of MEApv-D1R neurons following manipulations in an animal's motivational state, such as feeding or hormone interventions. These experiments will allow us to better understand how MEApv-D1R neurons are encoding the valuation of the relative risk versus reward of a stimulus during periods of competing incentive states. More broadly, this work invites further exploration as to how neural circuits are organized to provide animals with flexible and adaptable strategies for motivation and decision making.

Experimental methods

Animals

All experiments were approved in accordance to the guidelines of the Institutional Animal Care and Use Committee of the University of Washington. Drd1a$^{Cre/+}$ mice and Slc6a3$^{Cre/+}$ (DAT-Cre) mice have been characterized previously [46,75]. The Cre-dependent reporter strain, *Rosa26Sor*$^{fs\text{-}Tdt}$, was purchased from Jackson Laboratories (stock #007914). Approximately equal numbers of male and female mice were used for all experiments, with the exception of the resident-intruder assay, in which only male

mice were used. Mice were housed on a 12-hr light cycle and given *ad libitum* access to food and water. Behavioral mice were 8 weeks or older, and mice used for slice electrophysiology were 5-8 weeks old. Mice were group housed, with the exception of male mice which were singly housed 2-3 weeks prior to the resident-intruder assay. Mice were bred onto a C57BL/6 background, and mice used for social interaction assays were wild-type C57BL/6.

Viruses and neuronal tracers

All viruses were produced in house with tires of 1-3 x 10^{12} particles per mL as described[76]. RetroBeads were obtained from Lumafluor and injected with a Hamilton syringe (0.5µl/side).

Surgery

Mice were anesthetized with isoflurane and positioned on a stereotaxic alignment device (David Kopf instruments) before injection. Body temperature was maintained with a heating pad during surgery and 1.5-2% isoflurane was delivered continuously through a nose port. Injection coordinates were as follows: MEA_{PV}, from bregma in mm, A-P: -1.5; M-L: ±2.5, D-V: -5.6; BNST, from bregma in mm, A-P: 0.2, M-L: ±1.25, D-V: -4.25; VMH_{DM}, from bregma in mm, A-P: 1.15, M-L: ±0.5, D-V: -5.5; VTA, from bregma in mm, A-P: -3.15, M-L: ±0.5, D-V: -4.5. For *in vivo* ChR2 experiments, fiber optic cannulae were manufactured in house as described[77] and implanted unilaterally 0.5mm above the coordinates listed for viral injection. For microinfusion experiments, cannulae were implanted lateral to MEA_{PV} at M-L: ±2.4mm from bregma. Behavioral testing and

slice electrophysiology experiments began following a minimum of a 2 week surgical recovery period, with the exception of RetroBead and microinfusion surgeries in which recovery was only 1 week. Following behavioral testing, injection sites and fiber implant placements were confirmed using immunohistochemistry on collected brain tissue sections. Mice with mistargeted injections or implants were excluded from this study.

Immunohistochemistry

Primary antibodies were against GFP (mouse, 1:1000, Invitrogen A11120; or rabbit, 1:1000, Invitrogen A11122) c-Fos (rabbit 1:2000, Milipore ABE457) or TH (mouse, 1:1000, Milipore MAB318). Secondary antibodies were conjugated to DyLight488 or CY3 (1:250, Jackson Immunolabs). All staining was done on free-floating 30 µm sections (overnight primary incubations at 4℃).

Electrophysiology

Coronal brain slices (250 µm) were prepared from mice aged 5-8 weeks old in an ice slush solution containing (in mM): 92 NMDG, 2.5 KCl, 1.25 NaH_2PO_4, 30 $NaHCO_3$, 20 HEPES, 25 glucose, 2 thiouria, 5 Na-ascorbate, 3 Na-pyruvate, 0.5 $CaCl_2$, 10 $MgSO_4$, pH 7.3-7.4[78]. Slices recovered for ≤12 minutes in the same solution at 32° before recovering for an additional 45 minutes at room temperature in a solution containing (in mM): 92 NaCl, 2.5 KCl, 1.25 NaH_2PO_4, 30 $NaHCO_3$, 20 HEPES, 25 glucose, 2 thiouria, 5 Na-ascorbate, 3 Na-pyruvate, 2 $CaCl_2$, 2 $MgSO_4$. All solutions were continually bubbled with O_2/CO_2, and all recordings were made at 32° in ACSF (in mM: 126 NaCl, 2.5 KCl, 1.25 NaH_2PO_4, 1.2 $MgCl_2$, 10 glucose, 25 $NaHCO_3$, 2 $CaCl_2$) continuously

perfused over slices at a rate of ~2 ml/min. Whole-cell patch clamp recordings were made using Axopatch 700B amplifier (Molecular Devises) with filtering at 1 KHz using 4-6 MΩ electrodes filled with an internal solution containing (in mM): 130 K-gluconate, 10 HEPES, 5 NaCl , 1 EGTA, 5 Mg-ATP, 0.5 Na-GTP, pH 7.3, 280 mOsm. Light evoked synaptic transmission was induced with 5 ms light pulses delivered at a rate of 0.1 Hz from an optic fiber placed directly in the bath. To measure excitatory responses, cells were held in voltage-clamp mode at -60 mV. For inhibitory evoked responses, cells were held in voltage-clamp mode at 0 mV. CNQX (10 μM) and picrotoxin (100 nM) were bath applied to block excitatory and inhibitory responses, respectively. SKF 81,297 (10 μM) was perfused over the slices for approximately 2-3 minutes before recording its effect. Excitability was measured as the number of action potentials in response to current injections of varying amplitudes before and after drug application.

Fos Induction

Fos experimental mice were singly housed and placed into the behavioral box each day for 3 days prior to the experiment in order to acclimate them to handling and context. On test days, mice were exposed to various threat stimuli for 3-5 minutes. Mice were sacrificed 90 minutes following exposure to stimuli.

Fos-positive neurons were identified and counted using ImageJ software. Virally transduced D1R neurons and Fos-positive D1R neurons were counted by hand by an experienced investigator blind to condition.

Calcium Imaging Analysis

We concatenated calcium imaging videos relative to all the behaviors for each animal. To correct for lateral displacements of the brain and prevent motion induced artifacts, we applied frame-by-frame rigid-body registration using TurboReg plugin in ImageJ. In order to get a better contrast and to prevent the artefactual detection of ROIs along high-contrast borders, we cropped surrounding black borders after registration.

After motion correction and cropping of the concatenated videos, neurons were automatically detected using a Constrained Non-Negative Matrix Factorization method for microendoscopic data (CNMF-e). CNMF-e was also used to extract fluorescence traces of single neurons and get their denoised and deconvolved neural activity (dF). dF was used for all the analyses, unless otherwise noted.

For each neuron the average dF over the recorded period was calculated [mdF(y)].

For defining cell selectivity, neural activity of each cell was shuffled in time to generate a null distribution of Ca^{++} activity relative to behavioral epochs. A cell was considered active during the selected time bins for a behavioral stimulus if the average dF during the selected time bins exceeded a threshold value (threshold was defined as the multiple of the average activity of each cell at which no cell was considered active in the null distribution during the selected time bins [dfy = dF(y) - x*mdF(y) < 0, where y is an arbitrary cell and x an integer]).

The selection of the behavioral time bins proceeded as follow: the longest hidebox period for each behavioral stimulus was selected and cell activity was averaged across the selected periods. For the approach to robobug, predator odorant and male bedding, if an exploratory event lasting longer than 10 seconds was identified, calcium traces

from 5 seconds before to 5 seconds after the beginning of the approach event were averaged. Alternatively, the longest series of subsequent exploratory epochs was used. Active neurons across mice were then pooled to produce the pseudo-population showed in the Venn diagram.

To analyze the dynamics of the neural representation of avoidance and approach cells across animals, exemplar traces in a range of 20 seconds around the start of the behavioral epochs were z-scored and averaged.

Behavior

For all behavior, blue light stimulation parameters were 10 Hz, 5 ms, 3 seconds on, 3 seconds off. Experiments were conducted during the light cycle. Animals from each cohort were exposed to all of the following behavioral paradigms in the same order with at least one week of separation in between each. Only male mice from each cohort were tested in the resident-intruder assay.

Predator Odor: For the predator odor assay, mice were habituated for 3-4 days to a behavioral chamber with an odorant dish filled with clean cat litter and a hide box on the opposite side of the chamber. On the test day, mice were placed in the chamber for a 5 minute habituation period with an empty odorant dish, followed by a 5 minute test period with blue light stimulation in which the mice were exposed to an odorant dish filled with cat litter saturated in cat urine. Behaviors scored were time spent in hide box, total time sniffing the odorant dish, frequency of approaches of the odorant dish and latency to first approach of the odorant dish.

Robobug: For the robobug assay, mice were placed in a behavioral chamber to which they had been previously habituated. On the test day, mice were placed in the chamber for a 2 minute habituation period followed by a test period with blue light stimulation including a 30 second period in which the robobug was remotely activated. Mice remained in the chamber with the stationary robobug for an additional 2 minutes. Scored behavior included latency to investigate the robobug following the remote activation period, time spent in hide box, and total time investigating the robobug.

Resident-intruder: For resident-intruder encounters, resident mice were singly housed for at least two weeks, with a total of 7 days of no cage change, were sexually experienced, and were 3-4 weeks older than intruder mice, which were group housed. Encounters took place during the light cycle. Mice were allowed a 10 minute non-scored habituation period following connection to the fiber optic cable. Intruders were placed into the resident's home cage and the blue light was turned on. Encounters lasted for 20 minutes, and videos were hand scored by an experienced investigator blind to treatment. Behaviors scored were resident-initiated investigation, grooming, and fighting (which included attacking/mounting, high-speed chasing and nudging).

RTPP: For real-time place preference assay, mice were placed in a two-chambered arena with partial walls dividing the two sides that allowed for passage of the fiber optic cable. One side of the area had horizontal black and white stripes, while the other side had vertical stripes. One side was randomly assigned to be paired with blue light stimulation, while the other was unpaired. The assay lasted for 20 minutes.

Statistics

All statistical analyses were performed using Prism software (GraphPad). For comparison of two groups an unpaired Student's *t* test was used, except where noted. For comparison of multiple groups a one-way ANOVA was used, followed by Tukey's or Bonferroni's post hoc analysis. For comparison of two or more groups across treatment condition or time a two-way repeated measure ANOVA was used, followed by Bonferroni post-hoc analysis. Although we did not formally test for it, data distribution was assumed to be normal. The sample sizes were not determined based on calculation, but were similar to those previously reported related to our experimental assays[23,24,26].

References

1 Elliot, A. J. & Covington, M. V. Approach and avoidance motivation. *Educ Psychol Rev* **13**, 73-92, doi:Doi 10.1023/A:1009009018235 (2001).

2 Stein, M. B. & Paulus, M. P. Imbalance of approach and avoidance: the yin and yang of anxiety disorders. *Biol Psychiatry* **66**, 1072-1074, doi:10.1016/j.biopsych.2009.09.023

S0006-3223(09)01150-0 [pii] (2009).

3 Elliot, A. J. & Thrash, T. M. Approach and avoidance temperament as basic dimensions of personality. *J Pers* **78**, 865-906, doi:10.1111/j.1467-6494.2010.00636.x

JOPY636 [pii] (2010).

4 Skinner, B. F. The control of human behavior. *Trans N Y Acad Sci* **17**, 547-551 (1955).

5 Schneirla, T. C. Behavioral development and comparative psychology. *Q Rev Biol* **41**, 283-302 (1966).

6 Lang, P. J., Bradley, M. M. & Cuthbert, B. N. Emotion, attention, and the startle reflex. *Psychol Rev* **97**, 377-395 (1990).

7 Schlund, M. W. & Cataldo, M. F. Amygdala involvement in human avoidance, escape and approach behavior. *NeuroImage* **53**, 769-776, doi:10.1016/j.neuroimage.2010.06.058

S1053-8119(10)00916-X [pii] (2010).
8 Aupperle, R. L. & Paulus, M. P. Neural systems underlying approach and avoidance in anxiety disorders. *Dialogues Clin Neurosci* **12**, 517-531 (2010).
9 Campese, V. D. *et al.* The Neural Foundations of Reaction and Action in Aversive Motivation. *Curr Top Behav Neurosci* **27**, 171-195, doi:10.1007/7854_2015_401 (2016).
10 Olds, M. E. & Olds, J. Approach-avoidance analysis of rat diencephalon. *J Comp Neurol* **120**, 259-295 (1963).
11 Canteras, N. S. The medial hypothalamic defensive system: hodological organization and functional implications. *Pharmacol Biochem Behav* **71**, 481-491, doi:S0091305701006852 [pii] (2002).
12 Blanchard, R. J. & Blanchard, D. C. Attack and defense in rodents as ethoexperimental models for the study of emotion. *Prog Neuropsychopharmacol Biol Psychiatry* **13 Suppl**, S3-14 (1989).
13 Dielenberg, R. A. & McGregor, I. S. Defensive behavior in rats towards predatory odors: a review. *Neurosci Biobehav Rev* **25**, 597-609, doi:S0149763401000446 [pii] (2001).
14 Cohen, B. D., Brown, G. W. & Brown, M. L. Avoidance learning motivated by hypothalamic stimulation. *J Exp Psychol* **53**, 228-233 (1957).
15 Stellar, J. R., Brooks, F. H. & Mills, L. E. Approach and withdrawal analysis of the effects of hypothalamic stimulation and lesions in rats. *J Comp Physiol Psychol* **93**, 446-466 (1979).
16 Blanchard, D. C. & Blanchard, R. J. Innate and conditioned reactions to threat in rats with amygdaloid lesions. *J Comp Physiol Psychol* **81**, 281-290 (1972).
17 LeDoux, J. The amygdala. *Curr Biol* **17**, R868-874, doi:S0960-9822(07)01779-4 [pii]

10.1016/j.cub.2007.08.005 (2007).
18 Gross, C. T. & Canteras, N. S. The many paths to fear. *Nat Rev Neurosci* **13**, 651-658, doi:10.1038/nrn3301

nrn3301 [pii] (2012).
19 Kollack-Walker, S., Don, C., Watson, S. J. & Akil, H. Differential expression of c-fos mRNA within neurocircuits of male hamsters exposed to acute or chronic defeat. *J Neuroendocrinol* **11**, 547-559, doi:jne354 [pii] (1999).
20 Dielenberg, R. A., Hunt, G. E. & McGregor, I. S. "When a rat smells a cat": the distribution of Fos immunoreactivity in rat brain following exposure to a predatory odor. *Neuroscience* **104**, 1085-1097, doi:S0306452201001506 [pii] (2001).
21 Choi, G. B. *et al.* Lhx6 delineates a pathway mediating innate reproductive behaviors from the amygdala to the hypothalamus. *Neuron* **46**, 647-660, doi:S0896-6273(05)00347-8 [pii]

10.1016/j.neuron.2005.04.011 (2005).
22 Pardo-Bellver, C., Cadiz-Moretti, B., Novejarque, A., Martinez-Garcia, F. & Lanuza, E. Differential efferent projections of the anterior, posteroventral, and posterodorsal subdivisions of the medial amygdala in mice. *Front Neuroanat* **6**, 33, doi:10.3389/fnana.2012.00033 (2012).
23 Lin, D. *et al.* Functional identification of an aggression locus in the mouse hypothalamus. *Nature* **470**, 221-226, doi:10.1038/nature09736

nature09736 [pii] (2011).
24 Wang, L., Chen, I. Z. & Lin, D. Collateral pathways from the ventromedial hypothalamus mediate defensive behaviors. *Neuron* **85**, 1344-1358, doi:10.1016/j.neuron.2014.12.025

S0896-6273(14)01134-9 [pii] (2015).
25 Todd, W. D. *et al.* A hypothalamic circuit for the circadian control of aggression. *Nat Neurosci* **21**, 717-724, doi:10.1038/s41593-018-0126-0

10.1038/s41593-018-0126-0 [pii] (2018).
26 Hong, W., Kim, D. W. & Anderson, D. J. Antagonistic control of social versus repetitive self-grooming behaviors by separable amygdala neuronal subsets. *Cell* **158**, 1348-1361, doi:10.1016/j.cell.2014.07.049

S0092-8674(14)01039-3 [pii] (2014).
27 Unger, E. K. *et al.* Medial amygdalar aromatase neurons regulate aggression in both sexes. *Cell Rep* **10**, 453-462, doi:10.1016/j.celrep.2014.12.040

S2211-1247(14)01093-6 [pii] (2015).
28 Bian, X. Physiological and morphological characterization of GABAergic neurons in the medial amygdala. *Brain Res* **1509**, 8-19, doi:10.1016/j.brainres.2013.03.012

S0006-8993(13)00393-4 [pii] (2013).
29 Bian, X., Yanagawa, Y., Chen, W. R. & Luo, M. Cortical-like functional organization of the pheromone-processing circuits in the medial amygdala. *J Neurophysiol* **99**, 77-86, doi:00902.2007 [pii]

10.1152/jn.00902.2007 (2008).
30 Burnett, C. J. *et al.* Hunger-Driven Motivational State Competition. *Neuron* **92**, 187-201, doi:S0896-6273(16)30525-6 [pii]

10.1016/j.neuron.2016.08.032 (2016).
31 Hoebel, B. G., Avena, N. M. & Rada, P. Accumbens dopamine-acetylcholine balance in approach and avoidance. *Curr Opin Pharmacol* **7**, 617-627, doi:S1471-4892(07)00196-8 [pii]

10.1016/j.coph.2007.10.014 (2007).
32 Bromberg-Martin, E. S., Matsumoto, M. & Hikosaka, O. Dopamine in Motivational Control: Rewarding, Aversive, and Alerting. *Neuron* **68**, 815-834, doi:10.1016/j.neuron.2010.11.022 (2010).
33 Schultz, W. Behavioral dopamine signals. *Trends Neurosci* **30**, 203-210, doi:S0166-2236(07)00068-9 [pii]

10.1016/j.tins.2007.03.007 (2007).
34 Vincenz, D., Wernecke, K. E. A., Fendt, M. & Goldschmidt, J. Habenula and interpeduncular nucleus differentially modulate predator odor-induced innate fear behavior in rats. *Behav Brain Res* **332**, 164-171, doi:S0166-4328(17)30294-2 [pii]

10.1016/j.bbr.2017.05.053 (2017).
35 Ipser, J. C., Kariuki, C. M. & Stein, D. J. Pharmacotherapy for social anxiety disorder: a systematic review. *Expert Rev Neurother* **8**, 235-257, doi:10.1586/14737175.8.2.235 (2008).
36 Oleson, E. B. & Cheer, J. F. On the role of subsecond dopamine release in conditioned avoidance. *Front Neurosci* **7**, 96, doi:10.3389/fnins.2013.00096 (2013).
37 Jaber, M., Robinson, S. W., Missale, C. & Caron, M. G. Dopamine receptors and brain function. *Neuropharmacology* **35**, 1503-1519, doi:S0028390896001001 [pii] (1996).

38 Hernandez-Lopez, S., Bargas, J., Surmeier, D. J., Reyes, A. & Galarraga, E. D1 receptor activation enhances evoked discharge in neostriatal medium spiny neurons by modulating an L-type Ca2+ conductance. *J Neurosci* **17**, 3334-3342 (1997).
39 Marowsky, A., Yanagawa, Y., Obata, K. & Vogt, K. E. A specialized subclass of interneurons mediates dopaminergic facilitation of amygdala function. *Neuron* **48**, 1025-1037, doi:S0896-6273(05)00940-2 [pii]

10.1016/j.neuron.2005.10.029 (2005).
40 Scibilia, R. J., Lachowicz, J. E. & Kilts, C. D. Topographic nonoverlapping distribution of D1 and D2 dopamine receptors in the amygdaloid nuclear complex of the rat brain. *Synapse* **11**, 146-154, doi:10.1002/syn.890110208 (1992).
41 Guarraci, F. A., Frohardt, R. J. & Kapp, B. S. Amygdaloid D1 dopamine receptor involvement in Pavlovian fear conditioning. *Brain Res* **827**, 28-40, doi:S0006-8993(99)01291-3 [pii] (1999).
42 Greba, Q., Gifkins, A. & Kokkinidis, L. Inhibition of amygdaloid dopamine D2 receptors impairs emotional learning measured with fear-potentiated startle. *Brain Res* **899**, 218-226, doi:S0006-8993(01)02243-0 [pii] (2001).
43 Guarraci, F. A., Frohardt, R. J., Falls, W. A. & Kapp, B. S. The effects of intra-amygdaloid infusions of a D2 dopamine receptor antagonist on Pavlovian fear conditioning. *Behav Neurosci* **114**, 647-651 (2000).
44 Chung, A. S., Miller, S. M., Sun, Y., Xu, X. & Zweifel, L. S. Sexual congruency in the connectome and translatome of VTA dopamine neurons. *Sci Rep* **7**, 11120, doi:10.1038/s41598-017-11478-5

10.1038/s41598-017-11478-5 [pii] (2017).
45 Lein, E. S. *et al.* Genome-wide atlas of gene expression in the adult mouse brain. *Nature* **445**, 168-176, doi:nature05453 [pii]

10.1038/nature05453 (2007).
46 Heusner, C. L., Beutler, L. R., Houser, C. R. & Palmiter, R. D. Deletion of GAD67 in dopamine receptor-1 expressing cells causes specific motor deficits. *Genesis* **46**, 357-367, doi:10.1002/dvg.20405 (2008).
47 Madisen, L. *et al.* A robust and high-throughput Cre reporting and characterization system for the whole mouse brain. *Nat Neurosci* **13**, 133-140, doi:10.1038/nn.2467

nn.2467 [pii] (2010).
48 Zhang, T. Y., Chretien, P., Meaney, M. J. & Gratton, A. Influence of naturally occurring variations in maternal care on prepulse inhibition of acoustic startle and the medial prefrontal cortical dopamine response to stress in adult rats. *J Neurosci* **25**, 1493-1502, doi:25/6/1493 [pii]

10.1523/JNEUROSCI.3293-04.2005 (2005).
49 Sanford, C. A. *et al.* A Central Amygdala CRF Circuit Facilitates Learning about Weak Threats. *Neuron* **93**, 164-178, doi:S0896-6273(16)30902-3 [pii]

10.1016/j.neuron.2016.11.034 (2017).
50 Choi, J. S. & Kim, J. J. Amygdala regulates risk of predation in rats foraging in a dynamic fear environment. *Proc Natl Acad Sci U S A* **107**, 21773-21777, doi:10.1073/pnas.1010079108

1010079108 [pii] (2010).
51 Beckett, S. R., Duxon, M. S., Aspley, S. & Marsden, C. A. Central c-fos expression following 20kHz/ultrasound induced defence behaviour in the rat. *Brain Res Bull* **42**, 421-426, doi:S0361923096003322 [pii] (1997).

52 Salchner, P. & Singewald, N. Neuroanatomical substrates involved in the anxiogenic-like effect of acute fluoxetine treatment. *Neuropharmacology* **43**, 1238-1248, doi:S0028390802003295 [pii] (2002).
53 Lee, H. *et al.* Scalable control of mounting and attack by Esr1+ neurons in the ventromedial hypothalamus. *Nature* **509**, 627-632, doi:10.1038/nature13169

nature13169 [pii] (2014).
54 Cadiz-Moretti, B., Otero-Garcia, M., Martinez-Garcia, F. & Lanuza, E. Afferent projections to the different medial amygdala subdivisions: a retrograde tracing study in the mouse. *Brain Struct Funct* **221**, 1033-1065, doi:10.1007/s00429-014-0954-y

10.1007/s00429-014-0954-y [pii] (2016).
55 Keshavarzi, S., Sullivan, R. K., Ianno, D. J. & Sah, P. Functional properties and projections of neurons in the medial amygdala. *J Neurosci* **34**, 8699-8715, doi:10.1523/JNEUROSCI.1176-14.2014

34/26/8699 [pii] (2014).
56 Davis, M., Walker, D. L., Miles, L. & Grillon, C. Phasic vs sustained fear in rats and humans: role of the extended amygdala in fear vs anxiety. *Neuropsychopharmacology* **35**, 105-135, doi:10.1038/npp.2009.109

npp2009109 [pii] (2010).
57 Day, H. E., Masini, C. V. & Campeau, S. The pattern of brain c-fos mRNA induced by a component of fox odor, 2,5-dihydro-2,4,5-trimethylthiazoline (TMT), in rats, suggests both systemic and processive stress characteristics. *Brain Res* **1025**, 139-151, doi:S0006-8993(04)01301-0 [pii]

10.1016/j.brainres.2004.07.079 (2004).
58 Asok, A., Ayers, L. W., Awoyemi, B., Schulkin, J. & Rosen, J. B. Immediate early gene and neuropeptide expression following exposure to the predator odor 2,5-dihydro-2,4,5-trimethylthiazoline (TMT). *Behav Brain Res* **248**, 85-93, doi:10.1016/j.bbr.2013.03.047

S0166-4328(13)00189-7 [pii] (2013).
59 Fendt, M., Endres, T. & Apfelbach, R. Temporary inactivation of the bed nucleus of the stria terminalis but not of the amygdala blocks freezing induced by trimethylthiazoline, a component of fox feces. *J Neurosci* **23**, 23-28, doi:23/1/23 [pii] (2003).
60 Soden, M. E. *et al.* Genetic Isolation of Hypothalamic Neurons that Regulate Context-Specific Male Social Behavior. *Cell Rep* **16**, 304-313, doi:10.1016/j.celrep.2016.05.067

S2211-1247(16)30680-5 [pii] (2016).
61 Flagel, S. B. *et al.* A selective role for dopamine in stimulus-reward learning. *Nature* **469**, 53-57, doi:10.1038/nature09588

nature09588 [pii] (2011).
62 Fadok, J. P. *et al.* A competitive inhibitory circuit for selection of active and passive fear responses. *Nature* **542**, 96-100, doi:10.1038/nature21047

nature21047 [pii] (2017).
63 Yang, H. *et al.* Laterodorsal tegmentum interneuron subtypes oppositely regulate olfactory cue-induced innate fear. *Nat Neurosci* **19**, 283-289, doi:10.1038/nn.4208

nn.4208 [pii] (2016).
64 Padilla, S. L. *et al.* Agouti-related peptide neural circuits mediate adaptive behaviors in the starved state. *Nat Neurosci* **19**, 734-741, doi:10.1038/nn.4274

nn.4274 [pii] (2016).
65 Silva, B. A. *et al.* Independent hypothalamic circuits for social and predator fear. *Nat Neurosci* **16**, 1731-1733, doi:10.1038/nn.3573

nn.3573 [pii] (2013).
66 Hari Dass, S. A. & Vyas, A. Copulation or sensory cues from the female augment Fos expression in arginine vasopressin neurons of the posterodorsal medial amygdala of male rats. *Front Zool* **11**, 42, doi:10.1186/1742-9994-11-42

1742-9994-11-42 [pii] (2014).
67 Bergan, J. F., Ben-Shaul, Y. & Dulac, C. Sex-specific processing of social cues in the medial amygdala. *Elife* **3**, e02743, doi:10.7554/eLife.02743 (2014).
68 McGregor, I. S., Hargreaves, G. A., Apfelbach, R. & Hunt, G. E. Neural correlates of cat odor-induced anxiety in rats: region-specific effects of the benzodiazepine midazolam. *J Neurosci* **24**, 4134-4144, doi:10.1523/JNEUROSCI.0187-04.2004

24/17/4134 [pii] (2004).
69 Martinez, R. C., Carvalho-Netto, E. F., Ribeiro-Barbosa, E. R., Baldo, M. V. & Canteras, N. S. Amygdalar roles during exposure to a live predator and to a predator-associated context. *Neuroscience* **172**, 314-328, doi:10.1016/j.neuroscience.2010.10.033

S0306-4522(10)01363-1 [pii] (2011).
70 Aaltonen, T. *et al.* Observation of s-channel production of single top quarks at the Tevatron. *Phys Rev Lett* **112**, 231803, doi:10.1103/PhysRevLett.112.231803 (2014).
71 Golden, S. A. *et al.* Persistent conditioned place preference to aggression experience in adult male sexually-experienced CD-1 mice. *Genes Brain Behav* **16**, 44-55, doi:10.1111/gbb.12310 (2017).
72 Ferrari, P. F., van Erp, A. M., Tornatzky, W. & Miczek, K. A. Accumbal dopamine and serotonin in anticipation of the next aggressive episode in rats. *Eur J Neurosci* **17**, 371-378, doi:2447 [pii] (2003).
73 Couppis, M. H. & Kennedy, C. H. The rewarding effect of aggression is reduced by nucleus accumbens dopamine receptor antagonism in mice. *Psychopharmacology (Berl)* **197**, 449-456, doi:10.1007/s00213-007-1054-y (2008).
74 Schultz, W. Multiple dopamine functions at different time courses. *Annu Rev Neurosci* **30**, 259-288, doi:10.1146/annurev.neuro.28.061604.135722 (2007).
75 Zhuang, X., Masson, J., Gingrich, J. A., Rayport, S. & Hen, R. Targeted gene expression in dopamine and serotonin neurons of the mouse brain. *J Neurosci Methods* **143**, 27-32, doi:S0165-0270(04)00350-4 [pii]

10.1016/j.jneumeth.2004.09.020 (2005).
76 Gore, B. B. & Zweifel, L. S. Genetic reconstruction of dopamine D1 receptor signaling in the nucleus accumbens facilitates natural and drug reward responses. *J Neurosci* **33**, 8640-8649, doi:10.1523/JNEUROSCI.5532-12.2013

33/20/8640 [pii] (2013).

77 Sparta, D. R. *et al.* Construction of implantable optical fibers for long-term optogenetic manipulation of neural circuits. *Nat Protoc* **7**, 12-23, doi:10.1038/nprot.2011.413 (2012).
78 Ting, J. T., Daigle, T. L., Chen, Q. & Feng, G. Acute brain slice methods for adult and aging animals: application of targeted patch clamp analysis and optogenetics. *Methods Mol Biol* **1183**, 221-242, doi:10.1007/978-1-4939-1096-0_14 (2014).

Supplemental

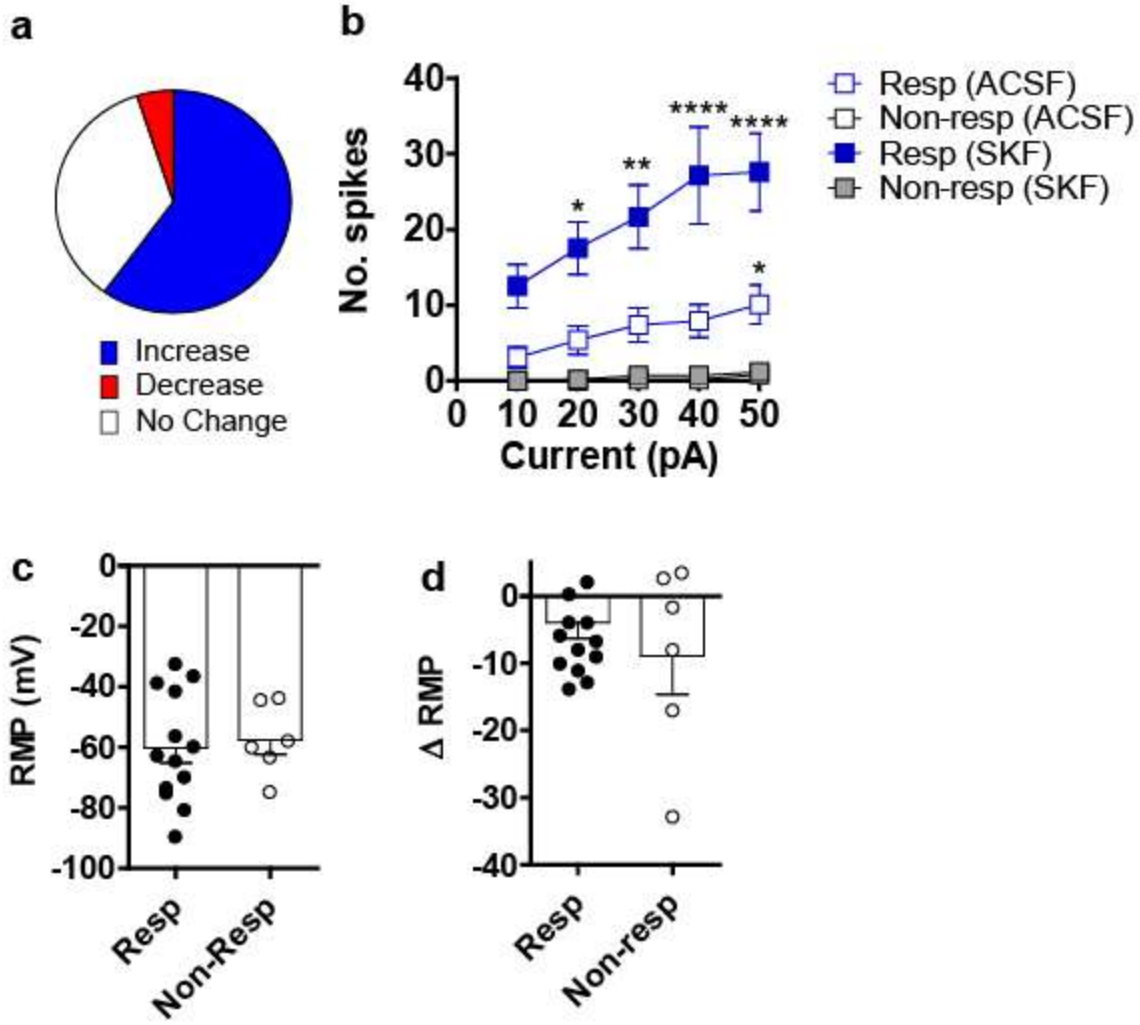

Figure 1: Effects of D1R agonist SKF 81,297 on excitability of MEApv-D1R neurons. (a) Pie chart of response to current injection following bath application of SKF 81,297 (14 of 20 increased, 6 of 20 no change, 1 of 20 decreased). (b) Number of action potentials (spikes) following current injection before (ACSF) and after SKF 81,207 application (2-way repeated measures ANOVA, $F_{(12,136)} = 3.12$, P = 0.0009, *P<0.05, **P<0.01, ****P<0.0001, Bonferroni multiple comparisons, responsive cells versus non responsive cells following SKF 81,297; 2-way repeated measures ANOVA, $F_{(4,68)} = 3.52$, P = 0.0113, *P<0.05, Bonferroni multiple comparisons, responsive cells versus non responsive cells during ACSF). (c) Resting membrane potential (RMP) was not different between responsive and non-responsive cells (P=0.7402, unpaired *t* test). (d) Change in resting membrane potential (□RMP) following SKF 81,297 perfusion was not different between responsive and non-responsive cells (P=0.3471, unpaired *t* test).

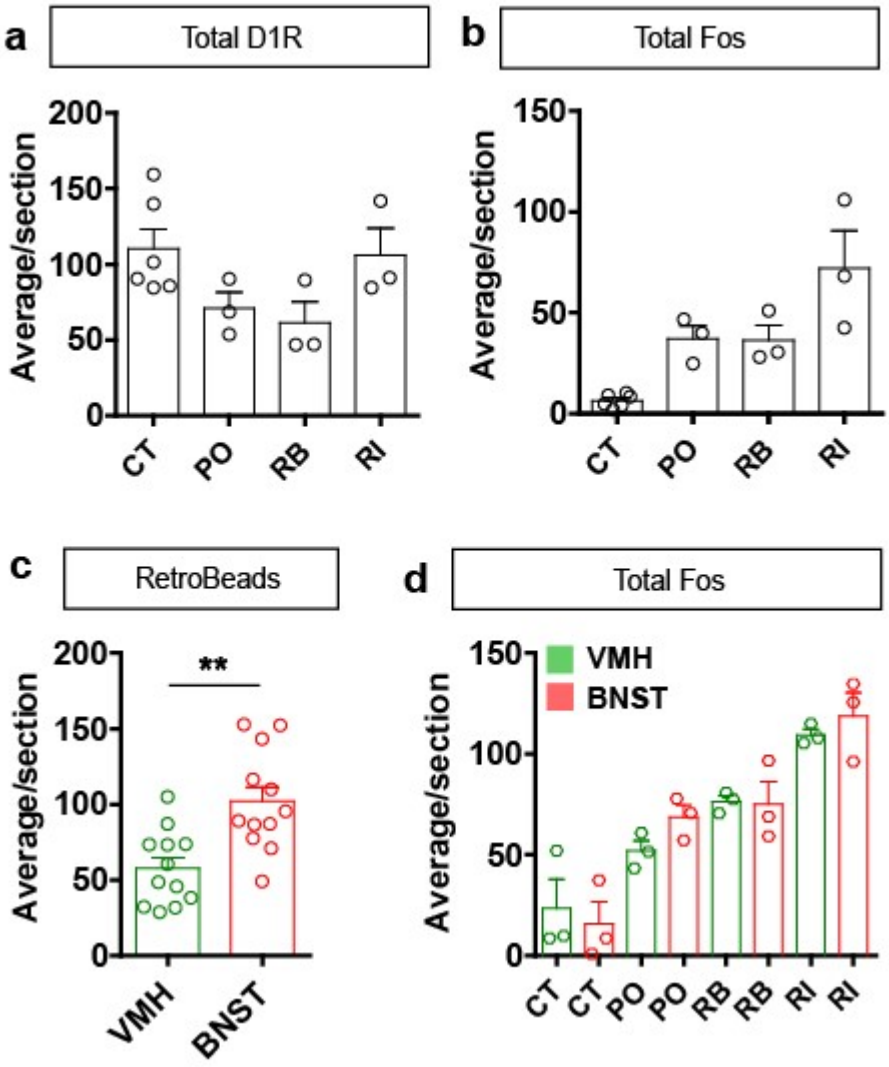

Figure2: Fos levels in the MEApv following exposure to different threats. (a) Total number of virally labelled MEApv-D1R neurons did not differ across assays. (b) Total Fos was significantly higher following predator odor (PO), robobug (RB), and resident-intruder (RI) assays (1-way ANOVA, $F_{(3,14)} = 12.31$, P = 0.008). (c) More neurons in the MEApv were labeled by RetroBeads injected into the BNST than into the VMH (P = 0.0012, unpaired *t* test). (d) Total Fos was significantly higher following predator odor (PO), robobug (RB), and resident-intruder (RI) assays following RetroBead injections into the BNST or VMH (2-way ANOVA, effect of assay $F_{(3,16)} = 35.56$, P < 0.0001).**

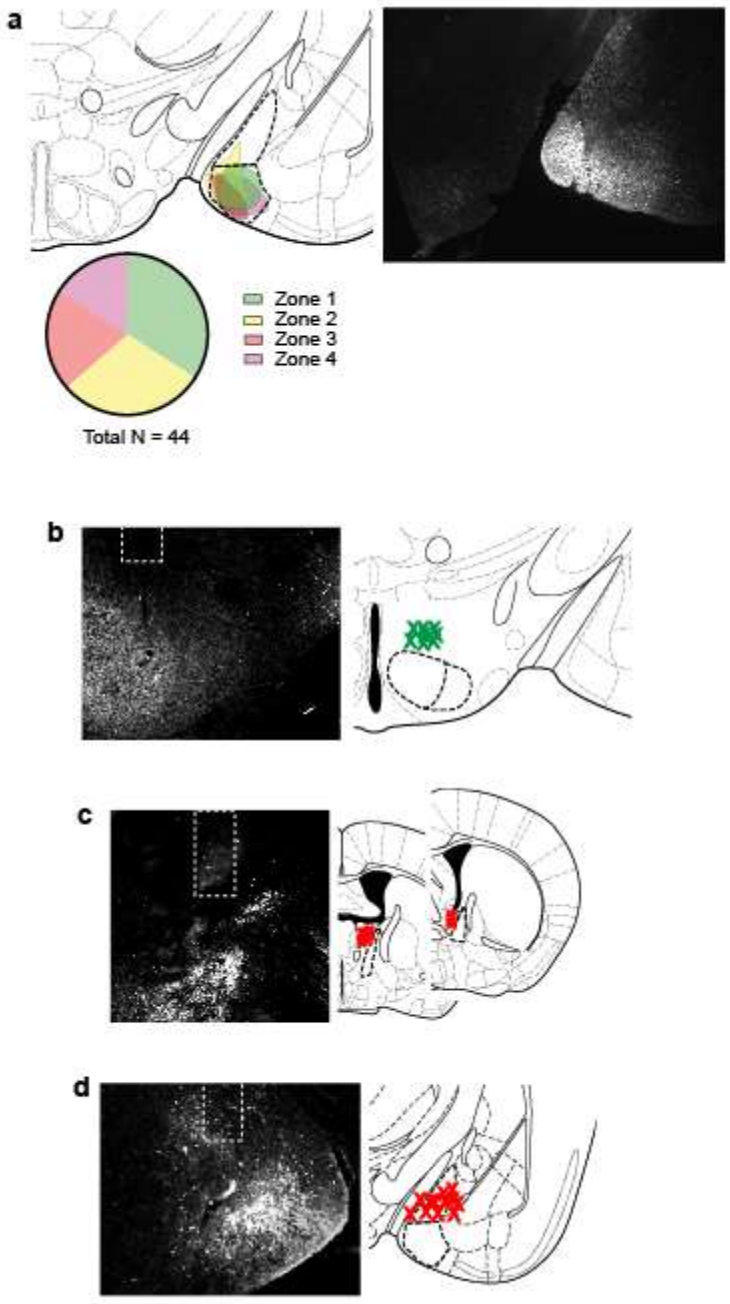

Figure 3: Confirmation of viral targeting and optical cannula placement. (a) Location of viral coverage designated as zones (1-4) within the MEApv for VMH terminal stimulation (b), BNST terminal stimulation (c) and MEApv cell body stimulation (d). Pie chart represents the distribution of virally labelling within the designated zones for the MEApv for each of the three experimental groups (N = 44 mice total for all three groups).

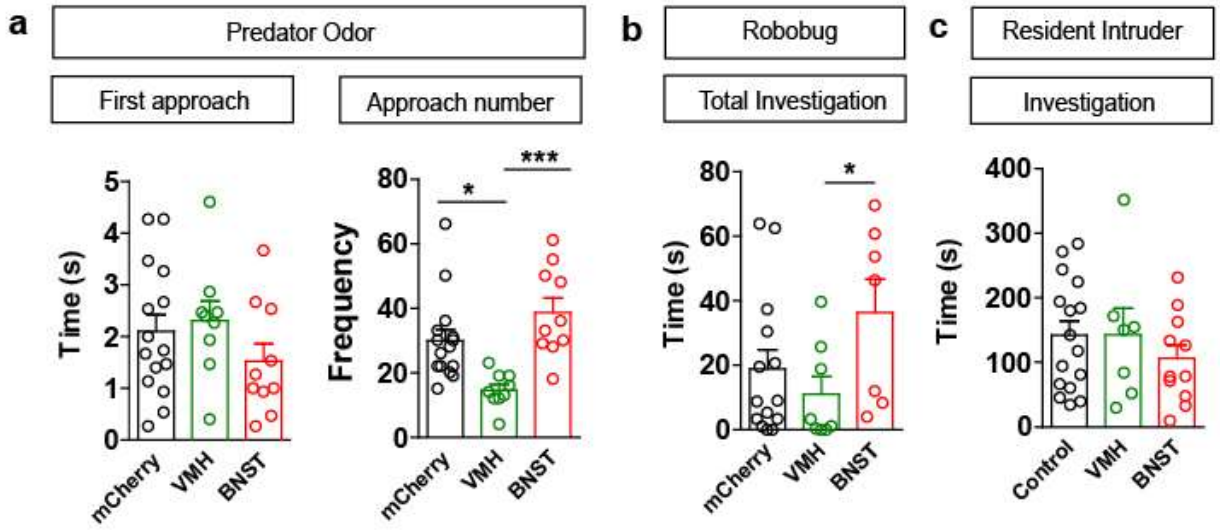

Figure 4: VMH and BNST projecting MEApv-D1R neurons oppositely regulate various behavioral responses to threat stimuli. (a) Activation of VMH and BNST projecting MEApv-D1R neurons does not affect latency to first approach the predator odor (n= 9-15 mice/group; 1-way ANOVA, $F_{(2, 31)}$=1.171, P = 0.3234). Activation of VMH projections from MEApv-D1R neurons significantly reduces frequency of approach (1-way ANOVA $F_{(2, 31)}$=9.992, ****P=0.0004, Tukey's multiple comparisons,*P<0.05, ***P<0.001) and activation of BNST projections from MEApv-D1R neurons increases sniffing time of predator odor (1-way ANOVA, $F_{(2, 31)}$= 16.87, ****P<0.0001, Tukey's multiple comparisons, ***P<0.001). (b) Compared to activation of VMH projections from MEApv-D1R neurons, activation of BNST projections from MEApv-D1R neurons increases time spent investigating robobug (n=7-14/group, 1-way ANOVA $F_{(2, 26)}$= 2.607, P=0.0929, Bonferroni's multiple comparisons, *P<0.05). (c) Activation of either VMH or BNST projections from MEApv-D1R neurons does not affect total investigation time of conspecifics in the resident intruder assay (n=7-16 mice/ group, 1-way ANOVA $F_{(2, 31)}$=0.6631, P=0.5224).

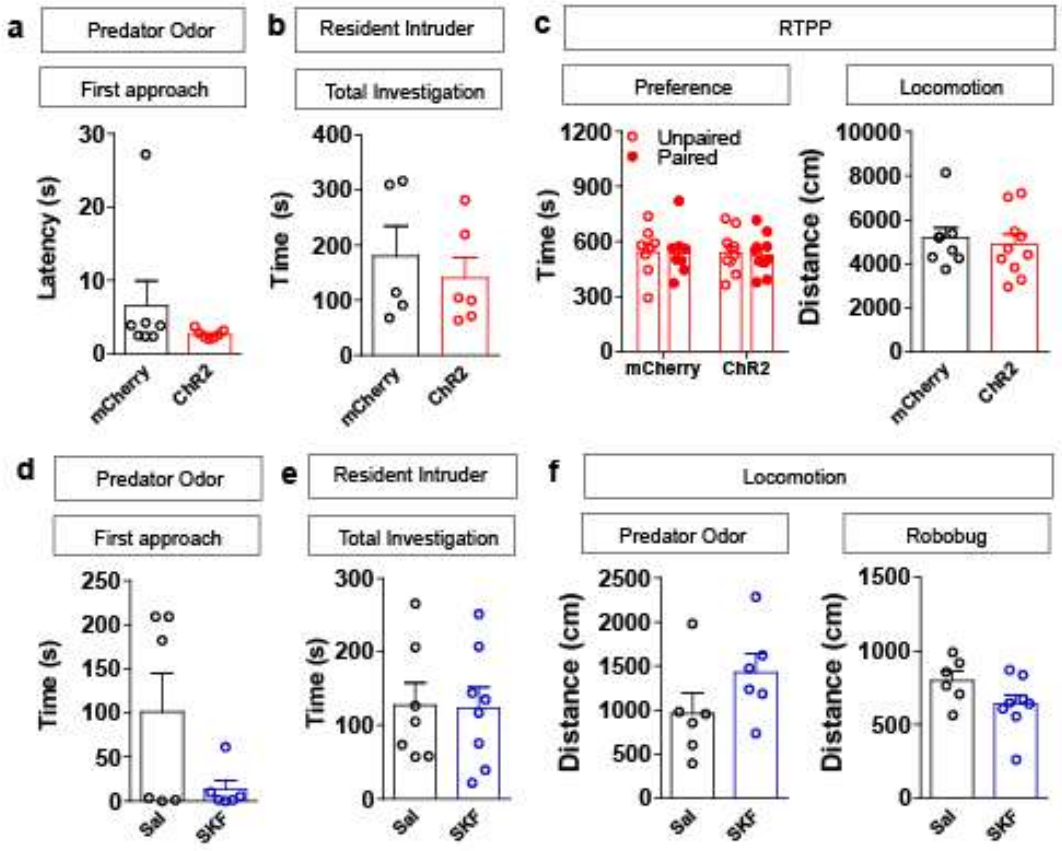

Figure 5: Activation of MEA$_{PV}$-D1R neurons does not affect some domains of defensive behavior. (a) Activation of MEApv-D1R neurons does not affect latency to first approach the predator odor container (n=7 mice/group, P=0.2745, unpaired *t* test) (b) Activation of MEApv-D1R neurons does not affect total time investigating the intruder mouse in the resident intruder assay (n=5-6 mice/group, P=0.5477, unpaired *t* test). (c) Activation of MEApv-D1R neurons does not elicit a real time place preference (n=8-10 mice/group, $F_{(1, 16)}$=0.03388, P=0.8563, 2-way ANOVA) and does not affect locomotor behavior (n=8-10 mice/group, P=0.6869, unpaired *t* test). (d) Infusion of SKF (3µg/0.5µl per side) does not significantly reduce latency to first approach predator odor (n=6 mice/ group, P=0.0833 unpaired *t* test) (e) Infusion of SKF does not affect social investigation of conspecifics in the resident intruder assay (n=7-8 mice/group, P=0.9331 unpaired *t* test). (f) Infusion of SKF does not affect locomotor behavior in either the predator odor assay (n= 6 mice/ group, P=0.1656 unpaired *t* test) or robobug assay (n= 6-8 mice/group, P=0.1088 unpaired *t* test).

Acknowledgments:

I first and foremost dedicate my dissertation to my most steadfast PhD companions, Pablo the Cat and Amanda Zila. And with all of my heart, I offer my deepest gratitude to all of the humans who supported me throughout this journey. In particular, Dr. Larry Zweifel and Dr. Marta Soden, I feel truly honored to have had the opportunity to train with the two of you. I look forward to many more years of learning from (and arguing with) you both for the rest of academic career.